Title
Biochemical Analysis of the COPII Coat Reveals Cargo Recruitment Is a Distinct Step from Vesicle Packaging

Author
Zhang, Peng Cheng

Publication Date
2015

Peer reviewed|Thesis/dissertation

Biochemical Analysis of the COPII Coat Reveals Cargo Recruitment Is a Distinct Step from Vesicle Packaging

By

Peng Cheng Zhang

A dissertation submitted in partial satisfaction of the

requirements for the degree of

Doctor of Philosophy

in

Molecular and Cell Biology

in the

Graduate Division

of the

University of California, Berkeley

Committee in charge:

Professor Randy Schekman, Chair
Professor David Bilder
Professor Gregory Barton
Professor Xiaohua Gong

Spring 2015

Abstract

Biochemical Analysis of the COPII Coat Reveals Cargo Recruitment Is a Distinct Step from Vesicle Packaging

by

Peng Cheng Zhang

Doctor of Philosophy in Molecular and Cell Biology

University of California, Berkeley

Professor Randy Schekman, Chair

The endomembrane system is the defining feature of eukaryotic cells and ensures that the appropriate proteins are sorted and transported to their correct subcellular location where they perform their biological functions. The coat protein complex II (COPII) mediates the formation of COPII vesicles, which are responsible for exporting proteins and lipids from the endoplasmic reticulum (ER). The core COPII coat consists of five proteins: the small GTPase Sar1, the Sec23/24 heterodimer, and the Sec13/31 heterotetramer. The recognition and subsequent packaging of cargo into COPII vesicles is mediated by interaction with the Sec24 subunit.

The development of a cell-free vesicle budding reaction has facilitated a biochemical analysis of COPII trafficking. Initial experiments examining COPII packaging of mammalian cargo proteins suggested that while some cargo proteins could be packaged directly by the core COPII components, other cargo proteins seemed to require additional cytosolic factors for efficient packaging. Whether auxiliary cytosolic factors exist to promote the COPII packaging of a specific subset of cargo proteins is the central question that motivated the work described in this dissertation.

This question was first approached using Vangl2, a cell surface localized transmembrane protein involved in planar cell polarity signaling, as a model cargo molecule. However, during the course of characterizing COPII packaging of Vangl2 *in vitro*, it was determined that this was not the appropriate system to address this question. As a result, proTGFα, the precursor form of transforming growth factor alpha, was chosen as a model cargo protein to continue to address the central question.

Here, I describe the key observations that show the existence of auxiliary cytosolic factor(s) that are required for efficient COPII packaging of specific cargo. In the particular case of proTGFα, both its recruitment by the COPII machinery and its final packaging into COPII vesicles require the cooperation of one or more auxiliary cytosolic factors and a transmembrane cargo receptor, Cornichon-1. Moreover, I present evidence showing that interaction of cargo proteins with the COPII coat is insufficient for packaging into COPII vesicles. This suggests that cargo recruitment and vesicle packaging are two distinct steps of COPII vesicle formation. Taken together, these

observations provide novel insights into the molecular mechanism of COPII vesicle formation in mammals.

Table of Contents

List of Figures

List of Tables

Acknowledgements

First of all I would like to thank my parents who have been a constant source of understanding, support and encouragement over the years.

I would like to thank the supporting staff at the Graduate Affairs Office for making bureaucracy as painless as it can be and for their timely reminders of other important stuff I need to do outside of lab.

I would like to thank all present and past members of the Schekman lab with whom I've had the pleasure of working. Thank you all for making my time in the lab such an enjoyable experience. I also enjoyed my many discussions with you about science and other topics.

I would especially like to express gratitude to Yusong Guo and Jason Lam, whose time in the lab almost completely overlapped with mine, and who have patiently provided all kinds of assistance to an unexperienced graduate student such as me.

I would like to thank Lazar Dimitrov and Lixon Wang for assistance in preparing HeLa CNIH knock out cells.

I would also like to thank our lab manager, Bob Lesch, who has pampered me with an extremely well managed lab. In addition, I would also like to thank Claudia Morales, our lab assistant who quietly ensures that we never run out of pipet tips and clean bottles or tubes.

I would like to thank the staff at the Tissue Culture Facility for making cell culture such a painless experience. I will indeed miss this privilege. Thank you, Ann Fischer, for running and maintaining such a fantastic facility!

I would like to thank my thesis committee for their advice and support over the years.

Last but not least, I would like to thank Randy for his patience, support and guidance throughout my time in the lab. Under Randy's mentorship, I learned how to think critically & independently, and how to ask scientific questions.

Chapter 1: Vesicular Trafficking and the COPII Coat

The Endomembrane System

The defining feature of the eukaryotic cell is its elaborate and dynamic endomembrane system which divides the cellular space into various membrane-bound organelles. In general, all eukaryotes have a nucleus, an endoplasmic reticulum, at least one Golgi apparatus, various endosomes, peroxisomes, and at least one lysosome (equivalent to the vacuole in yeast). All known extant eukaryotes also possess bona fide or relics of mitochondria (Embley and Martin, 2006), an organelle of endosymbiotic origin. Different eukaryotic cell types or organisms may possess more specialized organelles, such as secretory granules in professional endocrine cells or choloroplasts in plant cells.

The various intracellular organelles perform diverse biological functions that are critical for cell survival. For example, oxidative phosphorylation occurs in the mitochondria, while fatty acid synthesis occurs in the endoplasmic reticulum (ER). This achieves a spatial segregation of cellular function, which greatly enhances efficiency. The compartmentalization of the cell also allows for spatially restricting certain processes in distinct locales. For example, while the cytoplasm is a reducing environment, the ER lumen favors the formation of disulfide bonds. Another example is the difference of pH in different organelles: The lumen of the Golgi apparatus is more or less neutral, while the lysosome contains an acidic lumen. This ensures that proteinases are specifically activated when they arrive in the lysosome, and not in other organelles en route.

The endomembrane system is absolutely essential for achieving normal eukaryotic cellular functions. While the evolutionary origin of this system is yet to be determined (Williams et al., 2013), it is clear from extant eukaryotes that throughout evolutionary history, elaborate mechanisms have emerged to ensure the proper selection, targeting, and delivery of cellular proteins to the correct cellular locations where the proteins perform their normal biological functions (Dacks and Field, 2007; Field and Dacks, 2009).

There are many examples of localization signals encoded by the primary structure of the protein. For example, a nuclear localization sequence (NLS) is responsible for directing protein localization to the nucleus. Similarly, localization signals encoded in the primary structure of mitochondrial proteins synthesized in the cytoplasm can target the proteins to the mitochondria. Another well-characterized example is the co-translational translocation of newly synthesized peptides across the ER membrane, which is targeted by the signal sequence. These are all examples of targeted transport of cytosolic proteins to their respective destination organelles.

Additionally, many membrane-bound organelles can exchange material between one another through a process known as vesicular trafficking.

Vesicular Trafficking and the COPII Coat

Vesicular Trafficking

Vesicular trafficking refers to a process in which membrane bound organelles exchange lipids and protein via membrane enclosed vesicles. Vesicular trafficking has been suggested to occur in some prokaryotic cells (Huber et al., 2012; Nevo et al., 2007), but it is universal in all known eukaryotes and plays an essential role in maintaining protein homeostasis and cellular function.

In general, there are two directions of vesicular trafficking: retrograde and anterograde. If one imagines the nucleus and ER as more "internal" and the Golgi apparatus and endosomes & lysosomes as more "external", retrograde transport generally moves material from "external" to "internal", while anterograde transport moves material in the opposite direction.

Generally speaking, external protein is taken into the cell by endocytosis, forming an early endosome which then gradually matures into a late endosome. The late endosome usually further matures into a multi-vesicular body (MVB) and fuses with the lysosome, leading to the degradation of protein content. Proteins can also be recycled from the late endosome to the *trans*-Golgi network (TGN). Retrograde transport in the Golgi apparatus generally refers to transport from the *trans*-Golgi to the *cis*-Golgi, and from the *cis*-Golgi to the endoplasmic reticulum (ER).

Anterograde transport, in contrast, refers to the steps by which cells secrete proteins to the extracellular environment and therefore is also referred to as the secretory pathway. In this pathway, secreted or transmembrane proteins are synthesized at the ER and transported to the ER-Golgi intermediate compartment (ERGIC). The proteins then traverse the Golgi apparatus from *cis* to *trans* to reach the TGN, where they are sorted to diverse destinations such as recycling endosomes, late endosomes, or the plasma membrane.

The secretory pathway was characterized by the seminal work of George Palade (Caro and Palade, 1964). Subsequent decades of research have led to the discovery of molecular machinery which are responsible for vesicle generation at distinct and specific membranes (Babst et al., 2002a; Babst et al., 2002b; Balch et al., 1984; Bryant and Stevens, 1998; Kaiser and Schekman, 1990; Katzmann et al., 2001; Katzmann et al., 2003; Novick and Schekman, 1979; Novick et al., 1980; Pearse, 1976). The endoplasmic reticulum (ER) is the entry point of the secretory pathway. After completion of protein synthesis, proteins destined for transport are sorted and then packaged into vesicles in a process that is mediated by coat protein complex II (COPII).

The COPII Coat

The COPII coat consists of five subunits that are responsible for generating COPII vesicles that export protein and lipids from the ER. As depicted in Fig. 1.1, the process begins when the small GTPase, Sar1, is activated by the ER resident protein, Sec12. Sec12 acts as a guanine nucleotide exchange factor (GEF) and exchanges the GDP of inactive Sar1 for GTP (Barlowe and Schekman, 1993). GTP-bound Sar1 extends its N-terminal amphipathic loop and is recruited to the ER surface (Huang et al., 2001). At the ER surface, activated Sar1 recruits the Sec23/24 heterodimer, also termed the "inner coat". Sec24 is the COPII subunit responsible for recruiting transmembrane cargo proteins. The Sar1-Sec23/24-cargo intermediate is usually referred to as the "pre-budding complex". After the assembly of the pre-budding complex, the Sec13/31 heterotetramer, also called the "outer coat", is recruited to the nascent bud. The polymerization of

Sec13/31 provides the energy to induce membrane curvature and drive vesicle formation. After vesicle budding from the ER, Sec23, which acts as a GTPase activating protein (GAP), inactivates Sar1 by stimulating GTP hydrolysis. Sec31 further enhances the rate of GTP hydrolysis (Antonny et al., 2001; Antonny et al., 2003). GTP hydrolysis by Sar1 is thought to result in the disassembly of the COPII coat and its dissociation from the membrane for use in subsequent rounds of vesicle formation. The recruitment of cargo to the pre-budding complex, directly (via direct interaction between Sec24 and cargo) or indirectly (via cargo receptors), is the major mechanism for specific enrichment and packaging of cargo into nascent COPII vesicles.

A recent comparative genomic analysis suggested that the components of the COPII coat were likely present in the Last Eukaryotic Common Ancestor. Interestingly, the same analysis concluded that the Last Eukaryotic Common Ancestor had three Sec24 paralogs, and some paralogs were subsequently lost in certain eukaryotic lineages (Schlacht and Dacks, 2015). In the budding yeast *Saccharomyces cerevisiae*, where the *SEC* genes were originally identified, there are two non-essential paralogs in addition to the essential *SEC24*, known as *SFB2/ISS1* and *SFB3/LST1*. Lst1p was shown to be important for selective packaging of plasma membrane ATPase (Pma1p) in yeast (Roberg et al., 1999; Shimoni et al., 2000), while Iss1p was thought to play a specific role in the ER export of the v-SNAREs Sec22p & Bet1p and the glycolipid-anchored plasma membrane protein Gas1p (Kurihara et al., 2000; Peng et al., 2000).

In mammals, all core COPII components except Sec13 are present in the genome in at least two paralogous forms (Table 1.1). This genetic redundancy may reflect the need to process an increased repertoire of cargo that transits the secretory pathway. There is some evidence of Sec24 isoform dependent cargo specificity from animal studies. Sec24A knock out mice display low plasma cholesterol levels, a phenotype attributed to defective secretion of proprotein convertase subtilisin/kexin type 9 (PCSK9) (Chen et al., 2013). Sec24B defective mice display craniorachischisis, a severe neural tube defect, and this phenotype has been associated with defective cell surface delivery of Vang-like protein 2 (Vangl2), an important signaling protein in development (Merte et al., 2010; Wansleeben et al., 2010). Sec24D has been implied to play a role in the ER export of procollagen and bone & cartilage formation in zebrafish (Ohisa et al., 2010; Sarmah et al., 2010). However, it should be noted that there seems to be significant redundancy among the various mammalian Sec24 isoforms, and the number of cargo molecules that are known to be exclusively packaged by a specific Sec24 isoform is small. In genetic studies, single knock out of Sec24C and Sec24D in mice resulted in embryonic lethality (Adams et al., 2014; Baines et al., 2013), while Sec23B knockout mice suffered perinatal death due to pancreatic degeneration (Tao et al., 2012). Given the central importance of the COPII coat in cellular function and animal physiology, it is therefore not surprising that defects in many of the COPII genes have been associated with human disease (Table 1.1).

About This Dissertation

A fundamental question in the field of vesicular trafficking is how specific proteins are recognized and packaged into vesicles for transport. For many transmembrane COPII cargo proteins, this is achieved by direct interaction with the Sec24 subunit via specific amino acid sequences or structural motifs.

Previous work in the lab had established the central role of Sec24B in packaging Vangl2 (Merte et al., 2010). However, although significant efforts were made, direct interaction between Sec24B and Vangl2 was not detected. This led to the hypothesis that auxiliary cytosolic factors may be involved and act as adaptors to bridge Vangl2 and Sec24B.

Motivated by these previous observations, I began my work in the Schekman lab seeking to address the following central questions: Are there auxiliary cytosolic factors (i.e. cytosolic factors besides the known core COPII components) that are required for COPII mediated transport of a specific subset of cargo proteins? If they do exist, what are they and what is the mechanism of their function?

I started by following up on the previous work done on Sec24B and Vangl2. Chapter 2 describes efforts to test a possible candidate protein, Dishevelled, and attempts at identifying the putative factors using the cytoplasmic C-terminus of Vangl2. Chapter 2 also explains why Vangl2 was not the ideal model cargo to address the central questions.

I then turned to using another transmembrane cargo protein, proTGFα, as a model cargo protein to address the central questions. Chapter 3 describes the key observations confirming the existence of auxiliary cytosolic factors involved specifically in proTGFα trafficking, as well as further characterization of the molecular mechanisms of proTGFα sorting.

This dissertation describes the expected and unexpected challenges in the process of answering these central questions, the strategies and ideas employed (not all of them successfully) to overcome these obstacles, and the key observations and their biological significance. While not all of the initial questions have been answered, in the process of answering these questions new insights into the molecular mechanism of COPII cargo sorting and packaging have been gained that may require some revision of the current model.

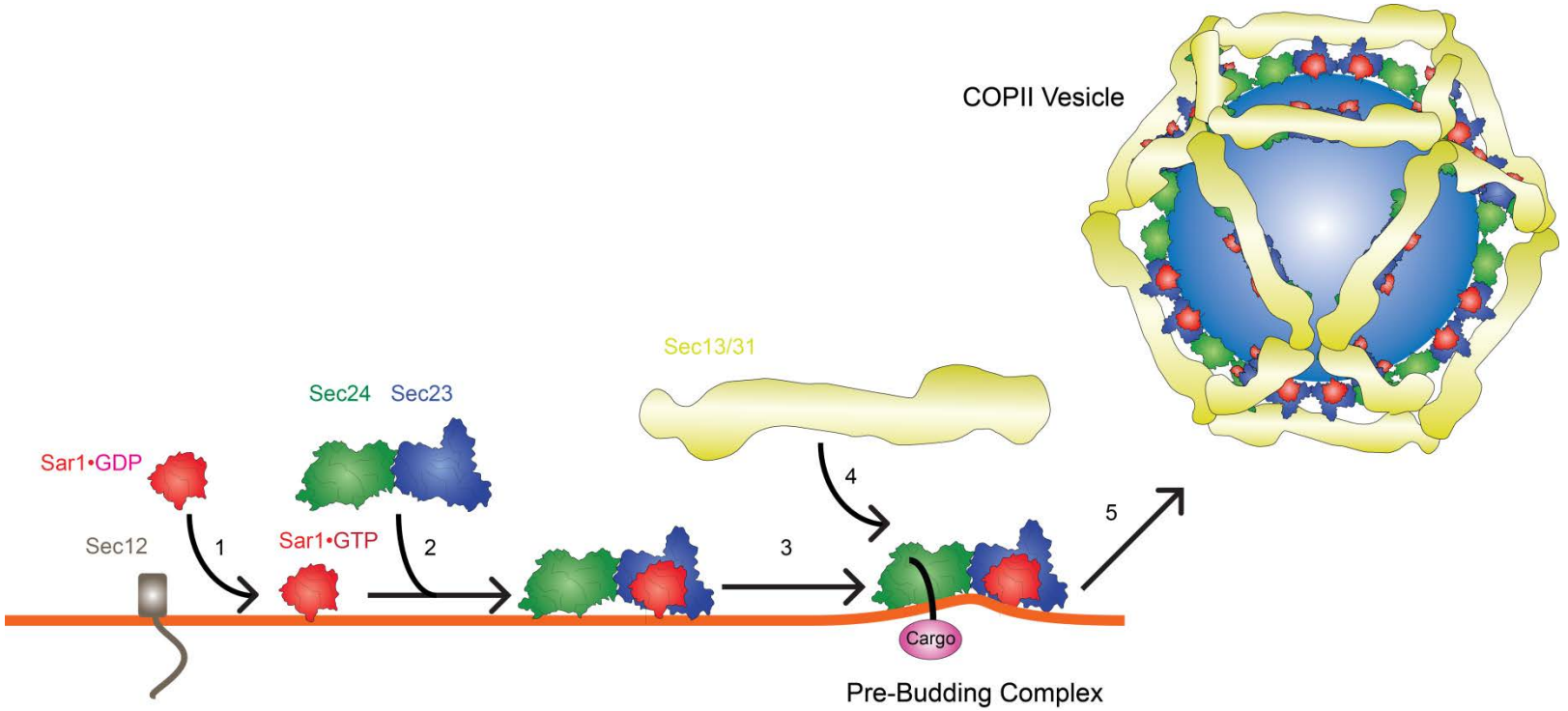

Figure 1.1 – Model of COPII Vesicle Formation
The ER resident protein Sec12 activates Sar1 by exchanging the bound GDP of inactive, cytosolic Sar1 for GTP, which activates Sar1 and allows it to associate with the ER membrane (1). Activated, GTP bound Sar1 recruits the Sec23/24 to the ER (2). The Sec24 subunit is primarily responsible for recognizing and recruiting appropriate cargo molecules to the pre-budding complex (3). After assembly of the pre-budding complex, the large Sec13/31 heterotetramer is then recruited to the ER (4), where it polymerizes and provides the driving force for inducing membrane curvature and leads to formation of nascent COPII vesicle (5).

Tables

Table 1.1 – COPII Paralogs and Disease

Yeast	Mammalian	Associated Disease	Reference
Sar1p	Sar1A		
	Sar1B	Chylomicron retention disease	(Jones et al., 2003)
Sec13p	Sec13		
Sec23p	Sec23A	Cranio-lenticulo-sutural dysplasia	(Boyadjiev et al., 2006; Lang et al., 2006)
	Sec23B	Congenital dyserythropoietic anemia, type II	(Bianchi et al., 2009; Schwarz et al., 2009)
Sec24p*	Sec24A		
Iss1p	Sec24B	Neural tube defect	(Yang et al., 2013)
Lst1p	Sec24C		
	Sec24D	Osteogenesis Imperfecta	(Garbes et al., 2015)
Sec31p	Sec31A		
	Sec31B		

* The order of the yeast Sec24 paralogs does not correspond to degree of sequence similarity to mammalian Sec24 homologs.

Chapter 2: *In Vitro* Characterization of COPII Packaging of Vangl2

Introduction

Planar Cell Polarity

Planar cell polarity (PCP) refers to the polarization of epithelial cells in the plane of the epithelium, in a direction that is orthogonal to apico-basolateral polarity. A set of core PCP genes was identified through genetic studies in *Drosophila melanogaster* to include the transmembrane proteins Frizzled (Fz/Fzd) (Gubb and García-Bellido, 1982; Vinson and Adler, 1987), Strabismus/Van Gogh (Stbm/Vang) (Taylor et al., 1998; Wolff and Rubin, 1998), & Celsr/Starry Night/Flamingo (Clsr/Stan/Fmi) (Usui et al., 1999), and the cytosolic proteins Dishevelled (Dsh/Dvl) (Axelrod et al., 1998; Krasnow et al., 1995), Diego (Dgo) (Feiguin et al., 2001) & Prickle (Prk) (Held et al., 1986).

In *Drosophila*, PCP signaling is important for the correct orientation of the fly eye (ommatidium), the polarized orientation of hair bundles (trichomes) on fly wings, and the orderly orientation of hair bristles on the fly thorax and legs.

In *Drosophila* wings, core PCP proteins are localized differentially to opposite sides of the cell (Seifert and Mlodzik, 2007; Simons and Mlodzik, 2008). Frizzled, a seven-pass transmembrane protein, is localized to the distal surface of *Drosophila* wing cells; while Vang, a four-pass transmembrane protein, is localized to the proximal surface. Flamingo is present on both the distal and proximal side, and is thought to function as a cell adhesion molecule. Frizzled interacts and recruits Dishevelled, which is thought to function as a scaffolding protein that recruits factors for downstream signaling. Interestingly, Dishevelled has also been shown to interact with Vang, which is localized at the opposite side of the cell.

Recent work in vertebrates has shown that PCP signaling seems to be largely conserved, although involved in different developmental processes (Curtin et al., 2003; Djiane et al., 2000; Etheridge et al., 2008; Hamblet et al., 2002; Jessen et al., 2002; Montcouquiol et al., 2003; Wallingford et al., 2000; Wang et al., 2006a; Wang et al., 2006b; Yu et al., 2012). It is essential for convergent extension and proper neural tube closure during vertebrate gastrulation, and in mammals proper PCP signaling is required for the correct development of the inner ear, or cochlea.

Vangl2

Vang-like 2, or Vangl2, is a homolog of *Drosophila* Van Gogh in mammals. Vangl2 is a four-pass transmembrane protein normally localized at the cell surface. It has two significant cytoplasmic domains in its N-terminus and C-terminus, and two very short extracellular loops (Fig. 2.1A). Two missense mutations in the cytoplasmic C-terminus of Vangl2, D255E & S464N have been linked to developmental defects in mice (Kibar et al., 2001a; Kibar et al., 2001b). Mice homozygous for either of the mutant Vangl2 alleles show severe neural tube closure defects, a condition called craniorachischisis in which the neural tube remains open from the hind brain to the most caudal end of the embryo. Not surprisingly, these homozygotes die before or shortly after birth. Heterozygotes which harbor one wild-type and one mutant allele display a much

milder phenotype, with a typical kink or loop in the tail. Thus these mutant forms of Vangl2 are called the Looptail mutants (Strong and Hollander, 1949). Vangl2 also contains a PDZ binding motif (PBM) at the end of its cytoplasmic C-terminus, which was shown to be important for gastrulation in vertebrates (Park and Moon, 2002) but seemed dispensable in *Drosophila* (Bastock et al., 2003). Missense mutations were found in the VANGL2 gene in stillborn or miscarried human fetuses which displayed neural tube defects (Lei et al., 2010), highlighting the essential role of Vangl2 in human development.

In a previous study from the lab in collaboration with the Ginty Lab at Johns Hopkins University, Vangl2 was shown to be preferentially selected for packaging into COPII vesicles by Sec24B (Merte et al., 2010). Additionally, it was shown that the Looptail mutants were defective for ER export. However, direct interaction between Vangl2 and Sec24b was not observed, raising the possibility that an additional auxiliary cytosolic factor(s) was required for COPII recognition of Vangl2 as a transport cargo. Additionally it was hypothesized that the reason the Looptail mutants were defective for trafficking was due to their inability to bind to this putative auxiliary factor.

Dishevelled

Dishevelled is a cytosolic protein with three conserved domains: an N-terminal DIX (Dishevelled, Axin) domain, a central PDZ (Postsynaptic density 95, Discs Large, Zona occludens-1) domain, and a C-terminal DEP (Dvl, Egl-10, Peckstrin) domain (Fig. 2.1B). It is an interaction partner of Vangl2 and has also been shown to function in convergent extension during vertebrate gastrulation (Wallingford et al., 2000). In mammals, there are three Dishevelled isoforms, Dvl1, 2, & 3. They exhibit some level of redundancy, as single knock-outs (KO) of any displays no or mild PCP phenotypes in mice (Etheridge et al., 2008; Hamblet et al., 2002; Lijam et al., 1997). Dvl2 KO mice show 2-3% neural tube defects, while Dvl1/Dvl2 double KO mice exhibit neural tube closure and cochlear defects. The other double KO combinations resulted in embryonic lethality, with Dvl2/Dvl3 double KO embryos already exhibiting neural closure defects as well as cardio outflow tract defects (Gao and Chen, 2010; Wang et al., 2006b). The involvement of Dishevelled in overlapping developmental processes and its interaction with Vangl2 raised the possibility that Dishevelled might function as the auxiliary cytosolic factor required for Vangl2 ER export.

Main Questions

The main questions I wanted to address are the following: Does ER export of Vangl2 require any auxiliary cytosolic factor(s) in addition to the core COPII components? Does Dishevelled function as an adaptor protein between Vangl2 and Sec24B and play a role in the ER export of Vangl2?

Materials and Methods

Antibodies

Anti-Sec22 antiserum was prepared as previously described (Merte et al., 2010). Anti-ERGIC53 antiserum was prepared as previously described (Fromme et al., 2007). Anti-Robophorin I antiserum was provided by Peter Walter. Anti-mouse and anti-rabbit HRP conjugates were from GE Healthcare UK (NXA931 and NA934V, respectively).

Rabbit anti-HA and Mouse anti-Myc monoclonal antibodies were from Cell Signaling (C29F4 and 9B11, respectively).

Materials

Rabbit muscle creatine phosphokinase, creatine phosphate, ATP, GTP and protease inhibitor mixture tablets were from Roche Applied Science. Rat liver cytosol was prepared as described previously (Kim et al., 2005). Trypsin with EDTA was from Invitrogen. Soybean trypsin inhibitor was from Fluka Biochemika. Micrococcal nuclease from *Staphylococcus aureus* was from USB-Affymetrix, dissolved in 50mM glycine, 5mM $CaCl_2$ at pH 9.2 and stored in 1 mg ml^{-1} aliquots. Digitonin was from Sigma and dissolved in DMSO at 40mg ml^{-1}.

Plasmid Construction

Vangl2-pCS2 plasmids harboring various point mutations were left behind by a previous graduate student (Jensen, 2010). The primers 5'-CTGAATTCGAGCTCCGTCAGCTCCAGCCC-3' and 5'-CTGTCGACTCACACAGAGGTCTCCGACTG-3' were used to amplify DNA corresponding to ammino acids 238-521 of Vangl2. The primers 5'-CTGAATTCATGGCGGAGACCAAAATCATC-3' and 5'-CTGTCGACTCAAAGCTGTGGGGCGCCAGGCAC-3' were used to amplify a region of mouse Dvl1 cDNA corresponding to amino acids 1-404. The primers 5'-CTGAATTCATGGCGGGCAGCAGCGCGGGG-3' and 5'-ctgtcgacTCAAGAGAGACCCCGGCCTTCGCAG-3' were used to amplify a region of mouse Dvl2 cDNA corresponding to amino acids 1-418. The primers 5'-CTGAATTCATGGGCGAGACCAAGATCATC-3' and 5'-CTGTCGACTCAGATGGAACTGGTGATGGAGGA-3' were used to amplify a region of human DVL3 cDNA corresponding to amino acids 1-395. The restriction enzymes *Eco*RI & *Sal*I were used to insert the PCR products into pGAD-C1 or pGBD-C1 plasmids (James et al., 1996) for use in yeast two-hybrid. The primers 5'-CCATCGATATGTCGGCCCCCGCCGGGTCC-3' and 5'-AGGTCGACTCACTTACAAACCTGCTGTTG-3' were used to amplify the full length of Sec24B cDNA. The PCR product was inserted into pGAD-C1 using the restriction enzymes *Cla*I & *Sal*I.

To construct pFastBac-GST, the glutathione S-transferase (GST) encoding region and multiple cloning site (MCS) region of a pGEX-4T-1 (GE Healthcare Life Sciences) plasmid was inserted into the MCS of pFastBac1 between the restriction sites of *Spe*I & *Not*I, and the original *Bam*HI and *Eco*RI sites of the pFastBac1 MCS were mutated via QuikChange to avoid redundancy with the same site in the MCS of pGEX-4T-1. Vangl2 C-terminus was inserted into pFastBac-GST between the restriction sites of *Eco*RI & *Hin*dIII.

Yeast Two-Hybrid Assay

The yeast strain PJ69-4a (James et al., 1996) was co-transformed with pGAD and pGBD plasmids using the well-established lithium acetate method (Gietz and Schiestl, 2007). Co-transformed yeast was plated on -LEU -TRP synthetic medium and incubated at 30°C until visible colonies were formed. Single colonies were then picked and

inoculated in -LEU -TRP synthetic medium and grown to saturation. Saturated yeast culture was then adjusted to the same optical density (at 600nm, OD_{600}=1.000) and serial dilution was performed (1:10, 1:100, and 1:1000 dilution of the original saturated culture). Each dilution (4μL) was then plated on -LEU -TRP (control), -HIS -LEU -TRP (low stringency), and -ADE -HIS -LEU -TRP (high stringency) plates, respectively, to assess protein interaction.

Purification of Recombinant Proteins

Human Sar1A H79G was purified as described (Kim et al., 2005). Human Syntenin-1 was purified according to the same procedures. Baculovirus were generated using the pFastBac-GST plasmids. Wild type (WT) or looptail (Lp255 and Lp464) GST-Vangl2 C-terminus (CT) were expressed in *Spodoptera frugiperda* (Sf9) cells by infecting Sf9 cells with baculovirus. At 72h post infection, Sf9 cells were harvested and lysed by sonication in lysis buffer (20mM HEPES, 10% glycerol, 250mM sorbitol, 500mM potassium acetate [KOAc], 0.1mM EGTA, 5mM β-mercaptoethanol [βME], 0.5% Triton X-100, pH 8.0). Cell debris was removed by centrifugation at 40,000 rpm in Type 45 Ti rotor (Beckman) for 1h at 4°C. The supernatant solution was then incubated with glutathione Sepharose resin (GE Healthcare Life Sciences), washed three times with lysis buffer, and eluted in elution buffer (20mM HEPES, 10% glycerol, 250mM sorbitol, 500mM KOAc, 0.1mM EGTA, 5mM βME, 0.5% Triton X-100, 25mM glutathione, pH 8.0). After elution, the most concentrated fractions were pooled and dialyzed into KHM buffer (20mM HEPES, 110 KOAc, 2mM magnesium acetate [MgOAc], pH 7.2) for use in budding reactions.

Preparation of Permeabilized Cells

The procedure for preparing permeabilized cells was performed as previously described (Merte et al., 2010).

***In Vitro* Translation**

In vitro translation was performed as previously described (Merte et al., 2010).

***In Vitro* Budding Reaction**

Vesicle formation and purification was performed as described previously (Kim et al., 2005), with slight modifications. In detail, donor membranes were incubated where indicated with rat liver cytosol, recombinant COPII proteins, ATP regeneration system, 0.3mM GTP, and Sar1A H79G. The reaction was carried out at 30°C for 1h, and terminated by incubation on ice for 5min. Donor membranes were removed by centrifugation at 14,000 *g* for 12min at 4°C. The resulting supernatant was centrifuged at 115,000 *g* for 25min at 4°C to collect COPII vesicles. Vesicle pellets were then resuspended in 15μL of Buffer C and Laemmli sample buffer. Vesicle samples and original donor membrane samples were resolved by SDS-PAGE, transferred on to PVDF membranes, and subjected to immunoblotting to detect various ER resident proteins and COPII cargo proteins.

Immunofluorescence Microscopy

Cos7 cells were grown on coverslips and transiently transfected with plasmids encoding HA-Vangl2 WT, Lp255, or Lp464 and Myc-Vangl2 using Lipofectamine 2000

according to the manufacturer's recommended protocol. Twenty hours later, cells were processed at room temperature for immunofluorescence microscopy according to the following protocol: Cells on coverslips were fixed in 4% paraformaldehyde (PFA) for 20min and washed three times with PBS. Cells were next permeabilized in Blocking Buffer (200mM glycine, 2.5% fetal bovine serum [FBS], 0.1% Triton X-100 in PBS) for 30min. Cells on coverslips were then incubated with the indicated primary antibodies diluted in Blocking Buffer for 30min and then washed three times with PBS. Subsequently, samples were incubated with secondary anti-rabbit or anti-mouse fluorescent conjugated antibodies diluted in Blocking Buffer for 30min and washed three times with PBS. Finally, coverslips were mounted on glass slides in ProLong Gold antifade mountant with DAPI (Life Technologies) and incubated at room temperature overnight in the dark. Slides were imaged using a Zeiss AxioObserver Z1 fluorescent microscope and images were captured using Metamorph software (Molecular Devices).

Results

Effects of C-Terminal Mutations on Vangl2-Dishevelled Interaction

Work done by a previous graduate student (Jensen, 2010) had examined the effects of point mutations in the cytoplasmic C-terminus of Vangl2 on its COPII packaging and subcellular localization (Table 2.1). The simple explanation is that the mutants are defective for ER export due to their defects in interaction with the putative auxiliary cytosolic factor(s). This would predict a correlation between protein-protein interaction and ER export.

Dishevelled is a well-characterized interaction partner of Vangl2 that also functions in the PCP pathway, which I considered as a possible candidate protein for the putative auxiliary cytosolic factor. To test this idea, yeast two-hybrid was employed to examine the interaction between Dishevelled and the cytoplasmic C-terminus of Vangl2 (Fig. 2.2-2.4). No significant difference in interacting patterns was observed between the different Dishevelled homologs (Compare Fig. 2.2-2.4), and on the whole the interaction pattern correlated reasonably well with ER export. The C-terminus of Vangl2 looptail mutants (D255E & S464N) displayed severe defects in binding to Dishevelled, which correlated with their inability to be packaged into COPII vesicles. Interestingly, when the same glycine residue (G256) was changed to different amino acid residues (G256V or G246N), the protein exhibited divergent behavior: Vangl2 G256V was defective for ER export, while Vangl2 G256N displayed normal trafficking and localization (Table 2.1). When analyzed in the yeast two-hybrid assay, Vangl2 CT G256V displayed weak interactions with all Dishevelled homologs, while Vangl2 CT G256N showed strong interactions comparable to WT levels (Fig. 2.2-2.4). A similar phenomenon was observed for S464. S464N is one of the looptail mutants and displays severe phenotypes *in vivo* and *in vitro*. However, when that same Serine residue is changed to Alanine, Vangl2 S464A shows WT localization & trafficking, and its C-terminus interacts with all three Dishevelled homologs similar at levels similar to that of the WT protein. Vangl2 CT W460A displayed slight reduction in interaction with Dishevelled, although the ER export of the full-length protein was disrupted.

Dishevelled Does Not Interact with Sec24B

Based on the observed correlation between Dishevelled binding and ER export, I hypothesized that Dishevelled may act as an adaptor protein linking Vangl2 to Sec24B. To test this hypothesis, I examined whether Dishevelled interacts with Sec24B, again using yeast two-hybrid.

No significant interaction was observed between Sec24B and any of the Dishevelled homologs (Fig. 2.5), while strong interaction was observed between Sec24B and its known interaction partner, Sec23B. The evidence so far did not support a role for Dishevelled as an adaptor protein for Vangl2 export, although an alternative possibility could be that the interactions in question are very transient and too weak to be detected by Y2H.

Addition of Vangl2 C-Terminal Fragments Inhibited Vangl2 Budding *In Vitro*

I concluded that this candidate approach was not conclusive, and sought to identify potential Vangl2 CT interaction partners using an affinity-based approach. The basic concept is to do GST pulldowns using GST-tagged Vangl2 CT and try to identify factors that preferentially bind to the WT protein by mass spectrometry.

However, before undertaking such an approach, I needed to ensure that the GST-tagged proteins are functional, which could be measured using the *in vitro* budding reaction. The idea is to add the soluble GST-tagged Vangl2 CT to the budding reaction and observe any competition between the soluble Vangl2 CT and the transmembrane Vangl2 on donor membranes. WT Vangl2 CT would be able to bind to the factors and compete with the transmembrane Vangl2 cargo for access to the trafficking machinery, while the looptail (Lp) mutants of Vangl2 CT would be defective for binding to the putative factors and therefore be unable to compete with the transmembrane Vangl2 cargo for access to COPII machinery. Thus I expected to observe inhibition of Vangl2 budding upon addition of GST-Vangl2 CT WT, whereas addition of GST-Vangl2 CT Lp would have no significant effect on Vangl2 trafficking. Additionally, I expected the effect of GST-Vangl2 CT on trafficking to be specific to Vangl2.

Rather unexpectedly, I found that wild type and mutant GST-Vangl2 CT inhibited Vangl2 budding *in vitro* (Fig. 2.6B). Addition of GST-Vangl2 CT also slightly inhibited the budding of other COPII cargo, such as Sec22.

The C-terminus of Vangl2 is known to oligomerize (Jensen, 2010), and oligomerized GST-Vangl2 CT could be sedimented by high speed centrifugation (data not shown). The reduction in Vangl2 budding *in vitro* could be due to the interference of Vangl2 C-terminal structure by GST-Vangl2 CT. Whatever the explanation, the observed phenomenon clearly contradicts my prediction, and strongly suggests that these purified GST-Vangl2 CT would not be useful to identify the putative cytosolic factor(s) using an affinity-based approach.

Vangl2 Looptail Mutants Can Alter the Localization of Vangl2 WT *In Vivo*

The failure to see specific inhibition of Vangl2 budding *in vitro* by addition of purified GST-Vangl2 CT raised the possibility that the trafficking defects of Vangl2 looptail mutants could be due to protein misfolding. Peculiarly, Lp255 consists of a single point mutation that changes an aspartate residue (D) to a glutamate residue (E), resulting in a difference of only one methyl group. Such a relatively conserved point mutation unexpectedly results in a near complete block of ER export. Moreover, both Lp

alleles behave in a dominant manner, as the presence of one mutant allele is sufficient to induce neural tube defects whereas the presence of both alleles leads to embryonic lethality or perinatal death.

To examine how Vangl2 looptail mutants affect wild-type Vangl2 localization *in vivo*, I co-transfected Cos7 cells with HA-Vangl2 (WT, Lp255, or Lp464) and Myc-Vangl2 WT. Subcellular localization of Vangl2 was then visualized by immunofluorescence microscopy using antibodies against either the HA or Myc epitope.

Consistent with the dominant nature of the looptail alleles, the Vangl2 looptail mutant proteins affected the localization of Vangl2 WT proteins when co-expressed in Cos7 cells (Fig. 2.7). Vangl2 WT normally localizes to the cell surface, but co-expression with either of the looptail mutants retains a significant amount of Vangl2 WT at the ER. Conversely, co-expression of the looptail mutants with the WT protein did not result in more localization of the looptail mutants at the cell surface (Fig. 2.7B & C). These observations suggest that Vangl2 does indeed interact with itself *in vivo* at the ER, and that either point mutation of the looptail mutants results in active retention of the protein at the ER, presumably due to improper folding.

Vangl2 Interacts with Syntenin

The last four residues in the C-terminus of Vangl2 (ETSV) constitute a PDZ binding motif (PBM). This motif was shown to be important for gastrulation in zebrafish (Park and Moon, 2002) but was found dispensable for protein function in *Drosophila* (Bastock et al., 2003). A previous graduate student in the lab had shown that a mutation of the C-terminal valine to glycine disrupted Vangl2 budding *in vitro* and resulted in the retention of Vangl2 in the ER (Table 2.1), implying a role for the PBM. Interestingly, Dishevelled binding to Vangl2, while dependent on the PDZ domain in Dishevelled, did not require the PBM on Vangl2 (Park and Moon, 2002).

I turned my attention to the mutations in the PBM of Vangl2, as mutations in this region occurred at the very C-terminus of the protein and was less likely to alter general structure. Syntenin is a cytosolic protein containing two tandem PDZ domains. It was a candidate of interest because it had been suggested to play a role in the early secretory pathway (Fernández-Larrea et al., 1999). Using yeast two-hybrid, I showed Vangl2 interacted with Syntenin and this interaction was dependent on the PBM of Vangl2 (Fig. 2.8). However, it should be noted that the interaction data did not correspond perfectly with *in vivo* localization data (Table 2.1), as the T519A mutation did not significantly affect Vangl2 localization, but abrogated Vangl2 interaction with Syntenin (Fig. 2.8). Despite this incongruence, it was nonetheless of interest to explore Syntenin's possible role in ER export.

Syntenin Does Not Function in Vangl2 ER Export

Human Syntenin-1 protein was purified and supplemented to *in vitro* budding reactions. As shown in Fig. 2.9, supplementing the reactions with Syntenin did not have any significant stimulatory effect on HA-Vangl2 budding. Although addition of 0.5μg of Syntenin seemed to slightly promote HA-Vangl2 budding compared to the other conditions, the level of HA-Vangl2 budding was not significantly higher than budding without addition of Syntenin. Notably, while Syntenin seemed to slightly inhibit HA-Vangl2 budding at higher amounts (1μg & 2μg), this effect was largely restricted to HA-

Vangl2 and did not affect the control cargoes ERGIC53 & Sec22. Therefore Syntenin did not seem to have a general effect on COPII budding. The evidence does not support a role for Syntenin in promoting Vangl2 trafficking from the ER.

Discussion

Vangl2 trafficking from the ER is dependent on the COPII coat. Previous work from this lab (Jensen, 2010), among others (Wansleeben et al., 2010), has shown the crucial role of the Sec24B subunit in the proper packaging of Vangl2 into COPII vesicles. Although the importance of Sec24B function has been established in the correct trafficking of Vangl2, the mechanism of cargo recognition and sorting seems not to be quite as straightforward. Although itself being a four-pass transmembrane protein, Vangl2 does not seem to be directly recognized by the COPII machinery, as direct interactions could not be established between Vangl2 and Sec24B. This prompted the hypothesis that an additional factor(s) was required, which likely served as a physical adaptor between Sec24B and Vangl2.

Using a yeast two-hybrid assay, a correlation between Vangl2-Dishevelled binding and Vangl2 trafficking could be observed. However, no direct interaction between Dishevelled and Sec24B was seen using this method. In fact, only Sec23B, a known strong interaction partner of Sec24B, could be demonstrated to interact with Sec24B using yeast two-hybrid. The cytosolic tail of other known COPII cargoes, such as VSV-G and Bet1, could not be demonstrated to interact with Sec24B as well (data not shown). This raised the question of whether the yeast two-hybrid assay was sensitive enough to detect the transient and weak interactions between Sec24 and cargo.

An alternative strategy was then devised, to make use of the cytoplasmic C-terminus (CT) of Vangl2 to identify interaction partners that preferentially interacted with the WT protein but not the looptail mutants. To confirm that the purified GST-tagged Vangl2 C-termini could interact with the putative factor(s), they were supplemented to *in vitro* budding reactions, with the expectation that GST-Vangl2 CT WT could specifically inhibit Vangl2 budding due to competition for the putative factor(s), while GST-Vangl2 CT Lp would be unable to specifically inhibit Vangl2 budding due to defect in binding. Unexpectedly, I saw inhibition of Vangl2 budding when any of the GST-Vangl2 CT constructs were supplemented to the *in vitro* budding reaction. Moreover, when elevated amounts of GST-Vangl2 CT were added to the reactions, a slight reduction in packaging of Sec22, a control cargo, was also observed. The most likely explanation for these observations could be the fact that Vangl2 CT is known to oligomerize. GST-Vangl2 CT could be sedimented by centrifugation at 100,000 *g* (data not shown), suggesting that it either oligomerizes to form large complexes in solution or associates with membranes. Oligomerization of GST-Vangl2 CT with full-length Vangl2 present at the ER membranes may induce the formation of relatively large protein clusters and render them unable to be packaged into COPII vesicles, thus explaining the decrease in Vangl2 budding. Large amounts of GST-Vangl2 CT may also associate with the membrane, and result in requirement of extra free energy to generate membrane curvature, thus explaining why elevated amounts of GST-Vangl2 CT in the budding reaction slightly reduces the budding of Sec22 as well.

That the Vangl2 looptail (Lp) mutants can alter the localization of Vangl2 WT *in vivo* is an indication that Vangl2 Lp is actively retained in the ER, rather than simply unable to exit the ER. Co-expression of Vangl2 Lp and Vangl2 WT in the same cell results in significant retention of Vangl2 WT in the ER, compared to expression of only Vangl2 WT. This suggests that Vangl2 does indeed oligomerize *in vivo* and may form clusters at the ER, presumably through its C-terminus. When co-expressed with Vangl2 WT in the same cell, Vangl2 Lp did not show a significant increase in cell surface localization, indicating that Vangl2 Lp is not simply sitting idle at the ER being ignored by the COPII coat (otherwise more Vangl2 Lp would be expected at the cell surface due to interaction with Vangl2 WT, which can be efficiently transported from the ER). Rather, Vangl2 Lp seems to be actively retained at the ER, and the retention of Vangl2 Lp at the ER overpowers the trafficking of Vangl2 WT from the ER, such that the looptail mutation is dominant over wild type, which is consistent with genetic evidence. Putting all the pieces together lends credence to the idea that looptail alters Vangl2 function and localization by disrupting protein structure, as had been proposed by others (Iliescu et al., 2011).

The focus of attention was then shifted towards the PDZ binding motif (PBM) at the very C-terminus of Vangl2. The PBM of Vangl2 had been shown to be required for the gastrulation of zebrafish embryos (Park and Moon, 2002), and the terminal valine was required for proper budding of HA-Vangl2 *in vitro* (Jensen, 2010). Mutation of residues at the very end of the polypeptide chain was less likely to induce general structural defects, and the V521G mutation did not result in complete retention of Vangl2 in the ER *in vivo*, displaying a milder phenotype compared to the looptail mutants.

Interaction was observed between Vangl2 C-terminus and Syntenin, a protein containing two tandem PDZ domains. Syntenin had previously been suggested to play a role in the early secretory pathway (Fernández-Larrea et al., 1999), but no functional evidence was provided. The observed interaction raised the prospect that Syntenin might play a role in ER export of Vangl2. This idea was tested *in vitro* by supplementing purified human Syntenin-1 protein to *in vitro* budding reactions. However, no significant effect on Vangl2 budding was observed, arguing against a role for Syntenin in this process.

Significant technical challenges prevented the further biochemical characterization of the cytosolic requirement for Vangl2 trafficking. Vangl2 is a transmembrane protein with complex topology and seemed to be prone to misfolding and/or aggregation. Overexpression of Vangl2 in cultured cells frequently resulted in retention of the wild type protein in the ER, and the ER-retained Vangl2 wild-type protein was deficient for budding *in vitro* (data not shown). To obtain detectable levels of Vangl2 budding *in vitro*, I resorted to *in vitro* translation and translocation to artificially insert the full-length protein into partially purified ER membranes (permeabilized cells) to obtain sufficient input. Even so, the budding efficiency of Vangl2 *in vitro* was consistently low, likely due to the structural instability resulting from relatively large protein size and complicated membrane topology, or aggregation due to *in vitro* protein synthesis in the absence of appropriate chaperones.

Whereas rat liver cytosol could support COPII budding from membranes prepared from almost any mammalian cell type, purified COPII proteins seemed much more sensitive to the species of membrane origin. The purified COPII proteins are all of human

origin, and past experience in the lab has shown that purified human COPII proteins could not support budding from membranes prepared from Chinese hamster ovary (CHO) cells, but could support budding from membranes harvested from HeLa cells, which are of human origin (Chris Fromme, personal communication). Artificial insertion of Vangl2 was most efficient when performed with Cos7 membranes. However, Cos7 cells were derived from kidney cells of the African green monkey *Cercopithecus aethiops*, and therefore Cos7 derived membranes were incompatible for use with purified COPII proteins *in vitro*. On the other hand, membranes prepared from HeLa cells and HEK293 cells displayed very inefficient protein insertion after *in vitro* translation, thus limiting the utility of Vangl2 as a model cargo protein to dissect the cytosolic requirements for COPII packaging.

In light of these technical hurdles, an alternative *in vitro* system was needed for teasing out the cytosolic requirements for COPII mediated trafficking. Additionally, Syntenin was originally identified as an interaction partner of proTGFα (Fernández-Larrea et al., 1999) and suggested to play a role in the ER export of proTGFα. As a result, I shifted my efforts to characterize proTGFα trafficking using HeLa membranes, which will be discussed extensively in Chapter 3.

Figures

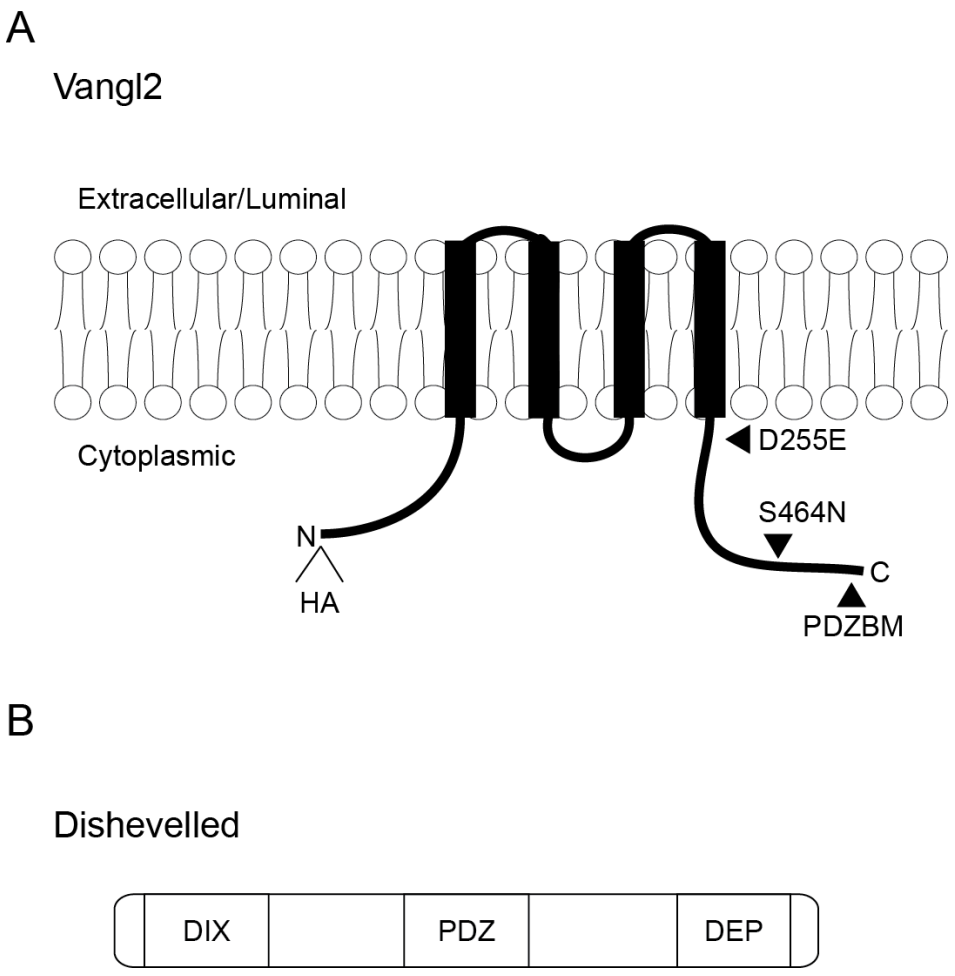

Figure 2.1 – Membrane Topology of Vangl2 and Domain Structure of Dishevelled
(A) Vangl2 is a four-pass transmembrane protein with two short extracellular loops and significant N-terminal and C-terminal cytoplasmic domains. Three tandem HA epitopes were fused to the N-terminus of Vangl2 for detection in immunoblots, and its position is indicated in the diagram. The positions of the two looptail mutations, D255E & S464N, are also indicated, as well as the PDZ binding motif (PBM). (B) Dishevelled contains three conserved domains: an N-terminal DIX domain, a central PDZ domain, and a C-terminal DEP domain. The PDZ domain is important for interaction with Vangl2.

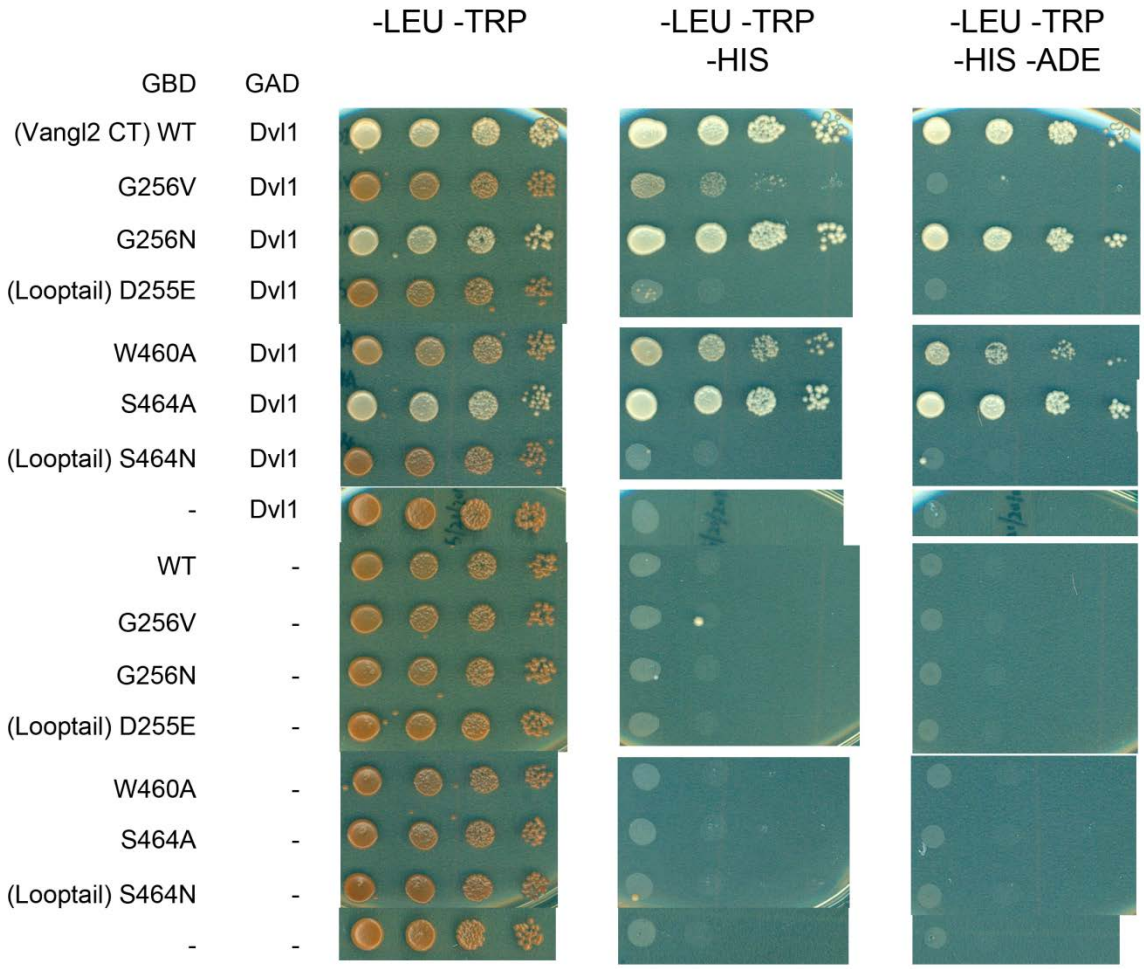

Figure 2.2 – Yeast Two-Hybrid Analysis of Interaction between Dishevelled 1 and the Cytoplasmic C-terminus of Various Vangl2 Mutants

Yeast two-hybrid analysis of interaction between Dishevelled 1 and Vangl2 C-terminus. PJ69-4A yeast was co-transformed with two plasmids expressing either Gal4 DNA binding domain (GBD) or Gal4 activating domain (GAD) fused to the indicated protein. Growth on -LEU -TRP -HIS plates indicated weak interaction between the protein combinations, while growth on -LEU -TRP -HIS -ADE plates indicated strong protein interaction. WT: Wild type.

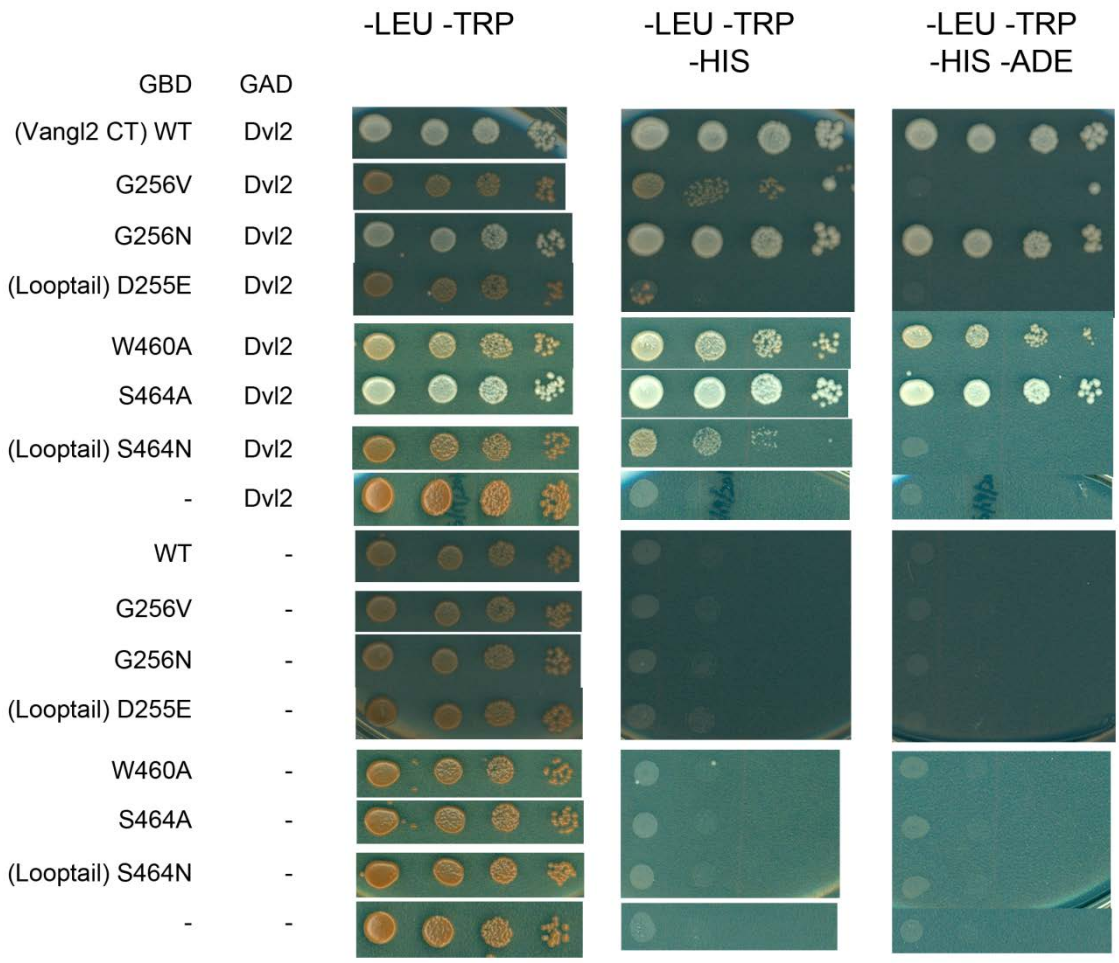

Figure 2.3 – Yeast Two-Hybrid Analysis of Interaction between Dishevelled 2 and the Cytoplasmic C-terminus of Various Vangl2 Mutants

Yeast two-hybrid analysis of interaction between Dishevelled 2 and Vangl2 C-terminus. PJ69-4A yeast was co-transformed with two plasmids expressing either Gal4 DNA binding domain (GBD) or Gal4 activating domain (GAD) fused to the indicated protein. Growth on -LEU -TRP -HIS plates indicated weak interaction between the protein combinations, while growth on -LEU -TRP -HIS -ADE plates indicated strong protein interaction. WT: Wild type.

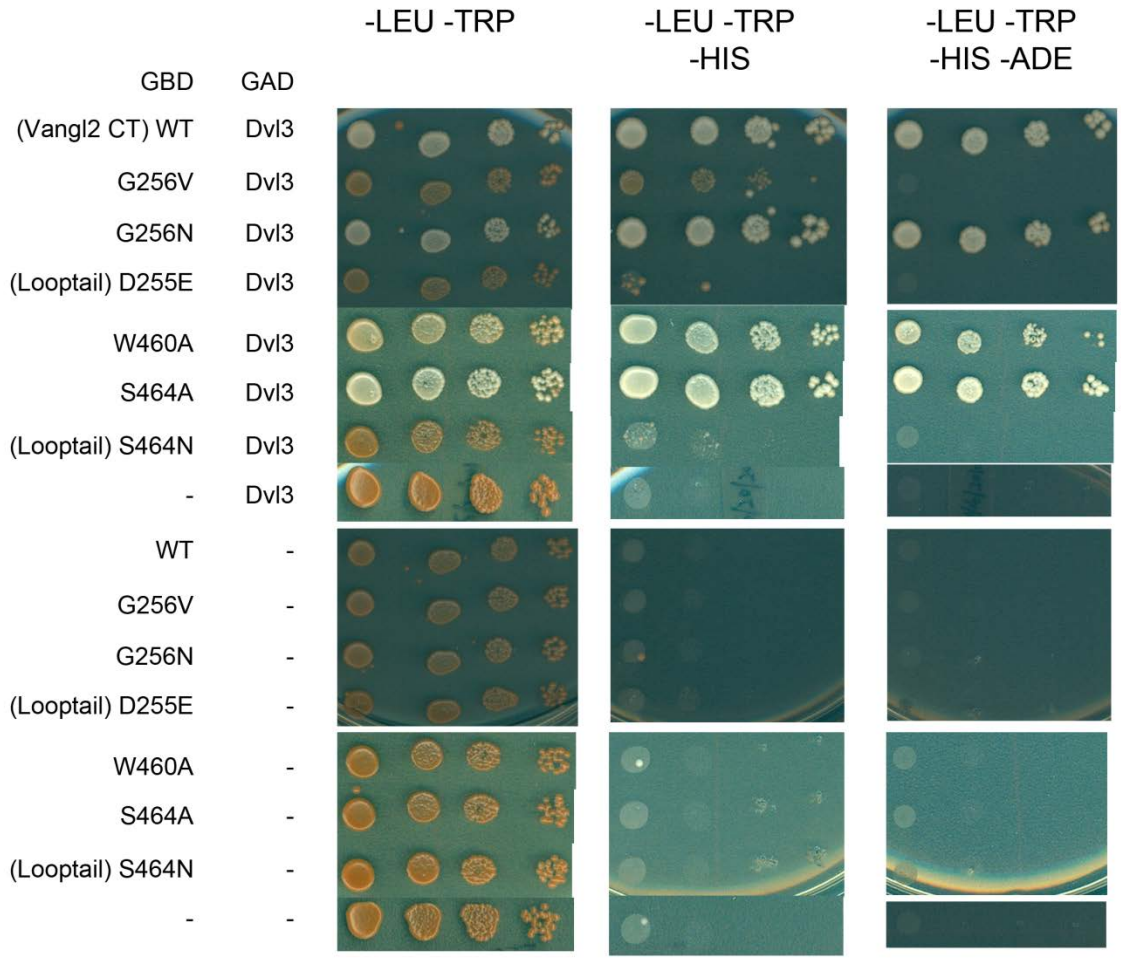

Figure 2.4 – Yeast Two-Hybrid Analysis of Interaction between Dishevelled 3 and the Cytoplasmic C-terminus of Various Vangl2 Mutants

Yeast two-hybrid analysis of interaction between Dishevelled 3 and Vangl2 C-terminus. PJ69-4A yeast was co-transformed with two plasmids expressing either Gal4 DNA binding domain (GBD) or Gal4 activating domain (GAD) fused to the indicated protein. Growth on -LEU -TRP -HIS plates indicated weak interaction between the protein combinations, while growth on -LEU -TRP -HIS -ADE plates indicated strong protein interaction. WT: Wild type.

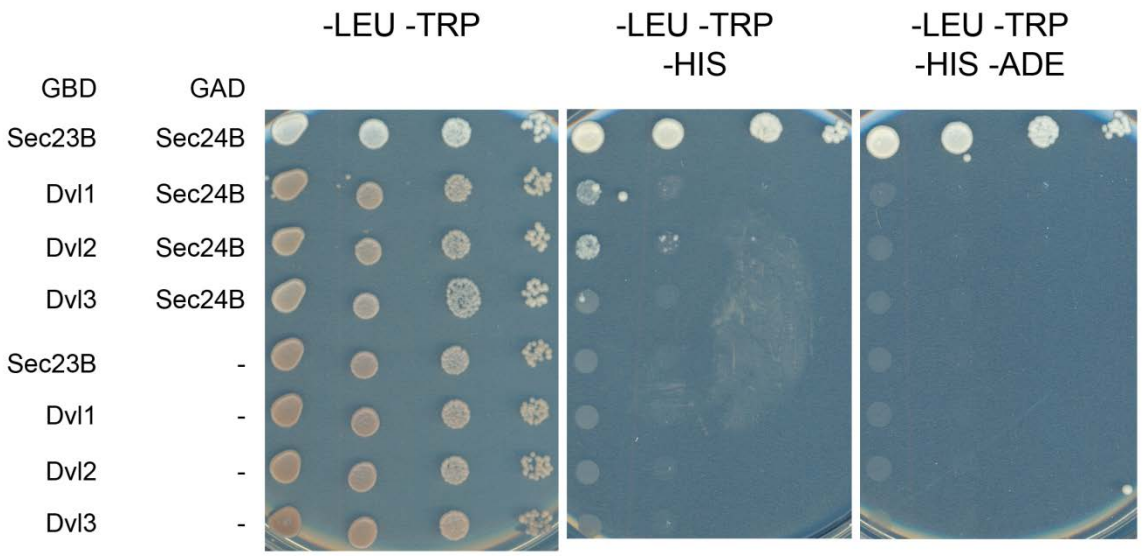

Figure 2.5 – Yeast Two-Hybrid Analysis of Interactions between Sec24B and Dishevelled Homologs

Yeast two-hybrid analysis of interactions between Sec24B and Dishevelled homologs. PJ69-4A yeast was co-transformed with two plasmids expressing either Gal4 DNA binding domain (GBD) or Gal4 activating domain (GAD) fused to the indicated protein. Growth on -LEU -TRP -HIS plates indicated weak interaction between the protein combinations, while growth on -LEU -TRP -HIS -ADE plates indicated strong protein interaction. Sec23B, a known interaction partner of Sec24B, was used as a positive control.

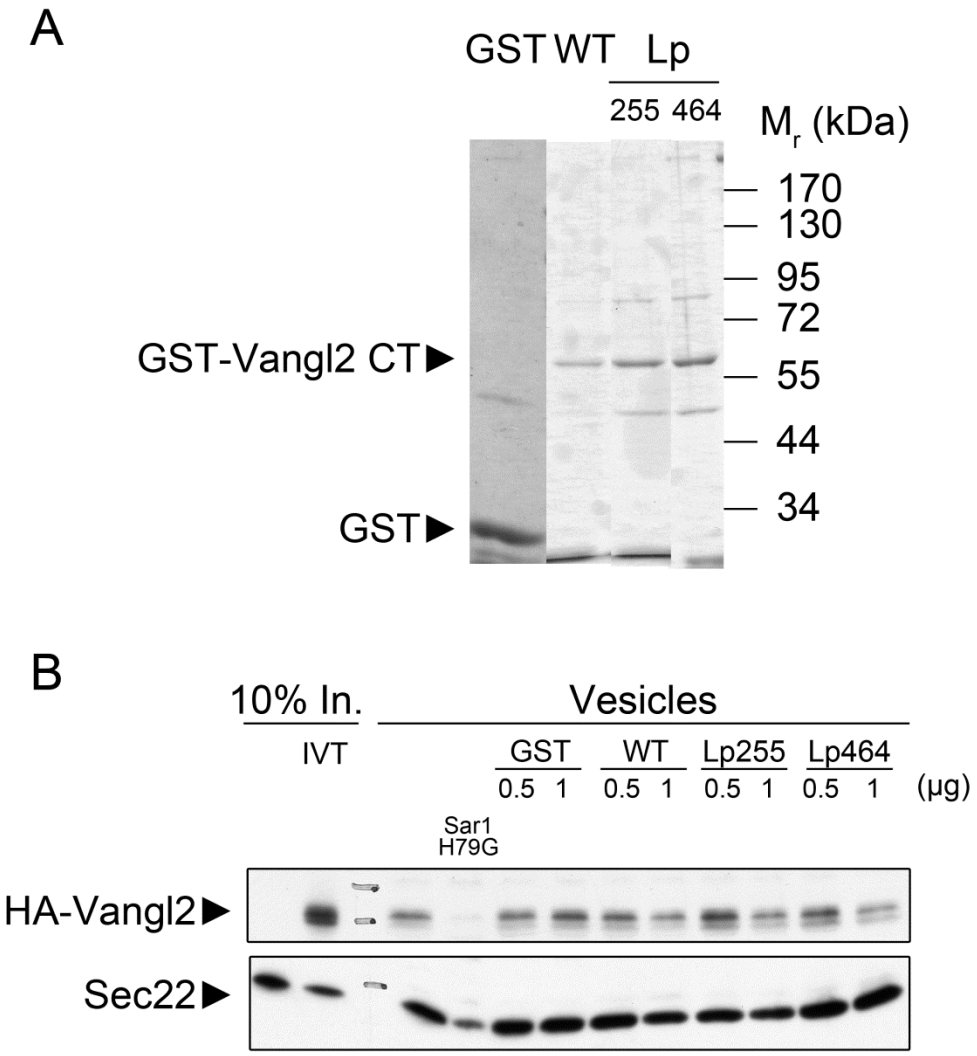

Figure 2.6 – Addition of GST-Vangl2 to *in vitro* Budding Reaction Inhibits HA-Vangl2 Budding

(A) Coomassie stain of purified GST, GST-Vangl2 CT WT, Lp255, and Lp464 as labeled. (B) Immunoblot of an *in vitro* budding reaction. Sar1 H79G acts as a dominant negative inhibitor of COPII budding *in vitro*. GST: Purified glutathione S-transferase. WT: Purified GST-Vangl2 CT WT. Lp255: Purified GST-Vangl2 CT D255E. Lp464: Purified GST-Vangl2 CT S464N. Addition of 1µg of any form of GST-Vangl2 CT resulted in significant reduction of HA-Vangl2 budding signal, and a slight reduction of Sec22 budding.

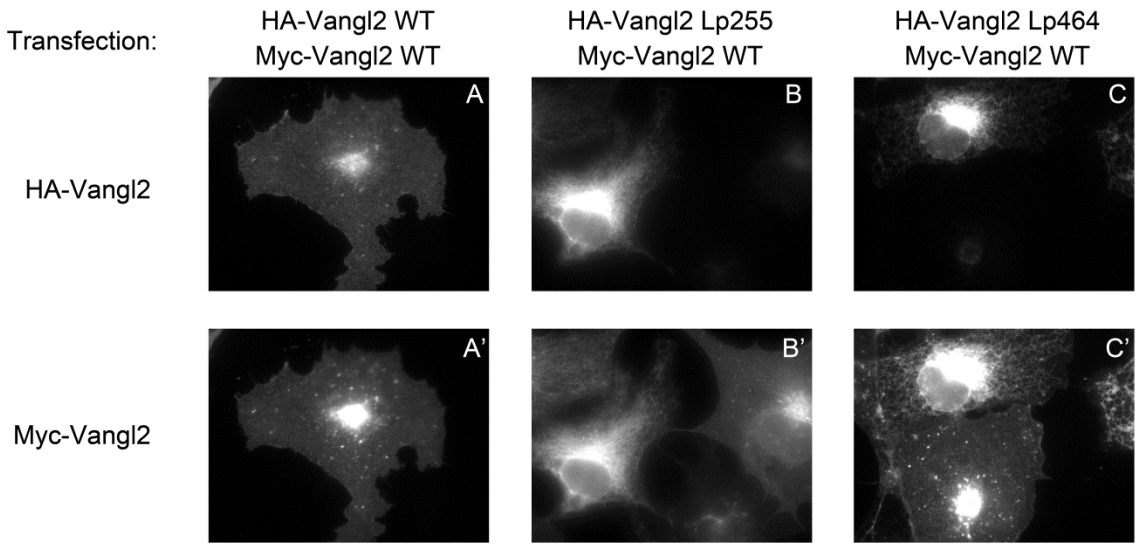

Figure 2.7 – Localization of Myc-Vangl2 and HA-Vangl2 in Co-Transfected Cos7 Cells

Cos7 cells were co-transfected with plasmids expressing Myc-Vangl2 WT and HA-Vangl2 WT, Lp255, or Lp464, and processed for immunofluorescence microscopy. Myc-Vangl2 and HA-Vangl2 were visualized using anti-Myc and anti-HA antibodies, respectively. (A) & (A') HA-Vangl2 WT and Myc-Vangl2 WT both displayed nice surface localization in co-transfected Cos7 cells. (B) HA-Vangl2 Lp255 displayed strong retention at the ER when co-expressed with Myc-Vangl2 WT. (B') Myc-Vangl2 WT localized primarily at the plasma membrane when expressed alone, but when co-expressed with HA-Vangl2 Lp255 displayed significant ER localization pattern. (C) HA-Vangl2 Lp464 localized nearly exclusively in the ER when co-expressed with Myc-Vangl2 WT in Cos7 cells. (C') Myc-Vangl2 WT showed significant ER localization pattern when co-expressed with HA-Vangl2 Lp464 in Cos7 cells.

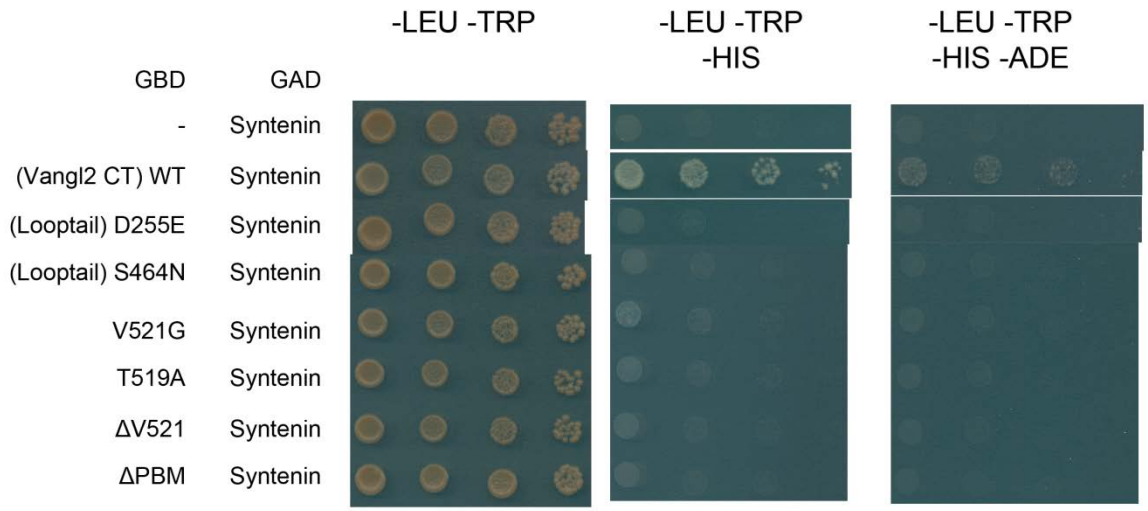

Figure 2.8 – Yeast Two-Hybrid Analysis of Interaction between Syntenin and the Cytoplasmic C-terminus of Vangl2

Yeast two-hybrid analysis of interactions between Syntenin and Vangl2 C-terminus. PJ69-4A yeast was co-transformed with two plasmids expressing either Gal4 DNA binding domain (GBD) or Gal4 activating domain (GAD) fused to the indicated protein. Growth on -LEU -TRP -HIS plates indicated weak interaction between the protein combinations, while growth on -LEU -TRP -HIS -ADE plates indicated strong protein interaction. WT: Wild type. ΔV521: Deletion of C-terminal valine. ΔPBM: Deletion of the entire PDZ binding motif (PBM).

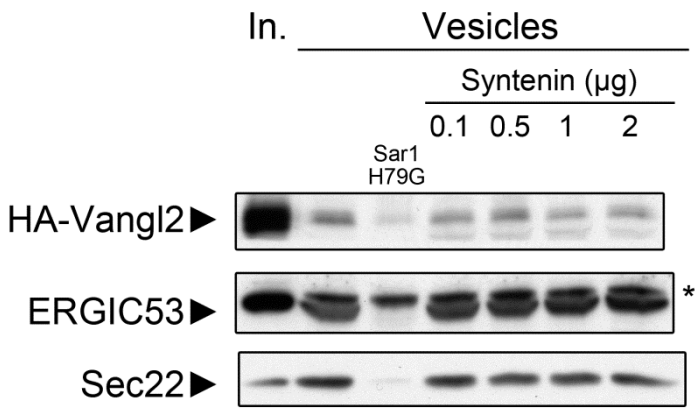

Figure 2.9 – Purified Syntenin Does Not Stimulate HA-Vangl2 Budding *In Vitro*
Human Syntenin-1 protein was purified from *E. coli* and supplemented at the indicated amounts to *in vitro* budding reactions. Addition of Syntenin did not stimulate budding of HA-Vangl2 above normal levels, and even seemed to slightly inhibit HA-Vangl2 budding at elevated levels. Sar1 H79G acts as a dominant negative inhibitor of COPII budding *in vitro*. Asterisk: non-specific band.

Tables

Table 2.1 – Effects of Select Mutations in Vangl2 C-Terminus on ER export

Vangl2 Construct	Surface Staining by Immunofluorescence	Packaging in COPII Budding Reaction
WT	++++	++++
D255E (Looptail)	-	-
G256V	-	-
G256N	++++	Not Tested
W460A	-	-
S464A	++	++
S464N (Looptail)	-	-
E518A	++++	Not Tested
T519A	++++	Not Tested
S520A	++++	Not Tested
V521G	+	-

Information was adopted from Devon Jensen's unpublished observations (Jensen, 2010).

Chapter 3: *In Vitro* Characterization of COPII Packaging of proTGFα

Introduction

proTGFα

Transforming growth factor alpha (TGFα) was identified as one of the secreted peptides from sarcoma virus-transformed fibroblasts that had cell transforming properties (de Larco and Todaro, 1978; Roberts et al., 1983; Todaro et al., 1976). It is a ligand of EGFR, and is thought to play a role in epithelial development. Mice with a null mutation of the TGFα gene display phenotypes including wavy hair, curly whiskers, and abnormal skin architecture, implying a role for TGFα in hair and skin development (Bunker and Snell, 1948; Crew, 1933; Green, 1989; Mann et al., 1993). The human TGFα gene was cloned in 1984 and was found to encode a transmembrane precursor protein of 160 amino acids (Derynck et al., 1984), termed proTGFα. The protein architecture consists of an N-terminal signal sequence followed by an ectodomain containing an EGF-like domain (the TGFα ligand), a transmembrane domain, and a C-terminal cytoplasmic tail (Fig. 3.1A). proTGFα contains sites for various post-translational modifications, including N-glycosylation (Teixidó et al., 1987) and O-glycosylation (Teixidó and Massagué, 1988) sites in the ectodomain, and palmitoylation sites (Shum et al., 1996) in the C-terminus. Newly synthesized proTGFα is glycosylated in the ER and then traverses the secretory pathway to reach the plasma membrane, where it undergoes two sequential proteolytic cleavages in its N-terminal extracellular domain to release the soluble TGFα into the extracellular space (Teixidó and Massagué, 1988; Teixidó et al., 1987).

The C-terminal cytoplasmic domain of proTGFα is short, only ~36 amino acids in length, but contains important determinants of intracellular trafficking (Briley et al., 1997; Ureña et al., 1999). The most C-terminal valine was characterized to be important for the ER export of proTGFα, and was recognized as part of a PDZ binding motif (PBM). Substitution of the terminal valine with other amino acid residues such as glycine (V160G) resulted in delayed ER export kinetics (Fernández-Larrea et al., 1999), while the steady state distribution of proTGFα V160G was similar to that of wild type when overexpressed in Chinese hamster ovary (CHO) cells. That the mutation occurs in the most C-terminal residue and the mutant protein still reaches the cell surface suggests that the trafficking defect is not due to protein misfolding.

Cornichon/Erv14p

Erv14p was identified in a proteinomics study of COPII vesicle components in the yeast *Saccharomyces cerevisiae* (Belden and Barlowe, 1996; Powers and Barlowe, 1998). In yeast, Erv14p functions as a transmembrane cargo receptor for Axl2p (Powers and Barlowe, 1998; Powers and Barlowe, 2002), among other potential transmembrane client proteins (Herzig et al., 2012; Nakanishi et al., 2007).

The *Drosophila* homolog of Erv14p was discovered through a genetic screen that identified a mutant in egg formation, and was named Cornichon (Roth et al., 1995). It was proposed that Cornichon normally functions as a cargo receptor to facilitate the ER export of Gurken (Bökel et al., 2006) similar to the role Erv14p plays in yeast.

Cornichon is a three-pass transmembrane protein with a cytoplasmic N-terminus and a luminal C-terminus (Fig. 3.1B). In yeast, Erv14p was found to interact with Sec24p via the cytoplasmic loop between the second and third transmembrane domains (Powers and Barlowe, 2002).

Interestingly, Gurken is a single-pass transmembrane protein that also contains a EGF-like domain in its extracellular region, and is also cleaved at the plasma membrane to release a soluble ligand into the extracellular space.

In vertebrates, there are four homologs of Cornichon: CNIH-1, CNIH-2, CNIH-3, and CNIH-4. CNIH-2 & CNIH-3 have been implicated in regulating the subunit composition of α-amino-3-hydroxy-5-methyl-4-isoxazolepropionic acid (AMPA) receptors in neurons (Herring et al., 2013). CNIH-4 has been shown to interact with newly synthesized G-protein coupled receptors (GPCRs) and is thought to play a role in their export from the ER (Sauvageau et al., 2014). In chick neural crest cells, CNIH-2 was shown to interact with HB-EGF, and was demonstrated to be important for HB-EGF secretion (Hoshino et al., 2007).

Interaction between proTGFα and CNIH-1 has been demonstrated, and the interaction domain on proTGFα has been mapped to the luminal EGF-like domain (Castro et al., 2007). A role for CNIH-1 in proTGFα trafficking from the ER has been proposed, but so far no functional studies have been carried out to examine this in detail.

Syntenin

A yeast two-hybrid screen using the cytoplasmic C-terminus of proTGFα as bait identified Syntenin-1 as an interaction partner (Fernández-Larrea et al., 1999). Syntenin is a cytosolic protein that contains two tandem PDZ domains (Fig. 3.1C). The C-terminal valine of proTGFα was mutated to various different amino acids and the various proTGFα constructs were tested for trafficking and maturation *in vivo*. Interestingly, Syntenin-1 was found to specifically interact only with the constructs that displayed normal trafficking kinetics (Fernández-Larrea et al., 1999). This gave rise to the idea that Syntenin-1 might be a required cytosolic factor to promote efficient ER export of proTGFα.

Main Questions

First I wanted to test whether Syntenin-1 had any function in the ER export of proTGFα. When *in vitro* data argued strongly against such a role for Syntenin-1, I next tried to determine whether proTGFα required any auxiliary cytosolic factor(s) at all.

I also wanted to further investigate the possibility that CNIH functions as a cargo receptor for proTGFα. The cytoplasmic C-terminal valine of proTGFα has been characterized to play an important role in ER export, whereas proTGFα interacted with CNIH in the ER lumen. These observations raise some interesting questions about the mechanism of cargo recruitment to the COPII pre-budding complex: Does proTGFα require an auxiliary cytosolic factor(s) for efficient recruitment? Does CNIH-1 play any role in proTGFα trafficking? What are the molecular mechanisms that mediate the sorting and packaging of proTGFα? These are the main questions that I will address in this chapter.

Materials and Methods

Antibodies

Anti-Sec13 and anti-Sec22 antisera were prepared as previously described (Merte et al., 2010). Anti-Sec23A, anti-Sar1A/B and anti-ERGIC53 antisera were prepared as previously described (Fromme et al., 2007). Anti-Sec31A monoclonal antibody was from BD Transduction Laboratories (612350). Anti-Ribophorin I antiserum was provided by Peter Walter. Anti-mouse and anti-rabbit HRP conjugates were from GE Healthcare UK (NXA931 and NA934V, respectively). Anti-HA monoclonal antibody was from Cell Signaling (C29F4). Anti-CNIH antibody was from Sigma (SAB1304796).

Materials

Rabbit muscle creatine phosphokinase, creatine phosphate, ATP, GTP and protease inhibitor mixture tablets were from Roche Applied Science. Rat liver cytosol was prepared as described previously (Kim et al., 2005). Trypsin with EDTA was from Invitrogen. Soybean trypsin inhibitor was from Fluka Biochemika. Micrococcal nuclease from *Staphylococcus aureus* was from USB-Affymetrix, dissolved in 50mM glycine, 5mM $CaCl_2$ at pH 9.2 and stored in 1 mg mL^{-1} aliquots. Digitonin was from Sigma and dissolved in DMSO at 40mg mL^{-1}.

Preparation of Permeabilized Cells

Procedure for preparing permeabilized cells and subsequent *in vitro* translation was performed as previously described (Merte et al., 2010), with slight modifications. In detail, HeLa cells were grown in a 100mm dish to 90% confluency, washed with PBS, trypsinized and washed again in KHM buffer containing 10μg mL^{-1} soybean trypsin inhibitor. Cells were then permeabilized in 40μg mL^{-1} digitonin for 5min in ice cold KHM buffer. Permeabilized cells were then washed once with B88-LiCl buffer, once in B88 buffer, and finally resuspended in B88 buffer, aliquoted, and stored at -80°C.
For use in *in vitro* translation, permeablized cells were washed once in KHM buffer after permeabilization with digitonin and resuspended in 100μL KHM buffer.

***In Vitro* Translation**

In vitro translation was performed as previously described (Merte et al., 2010), with slight modifications. In detail, 1mM $CaCl_2$ and 10μg mL^{-1} micrococcal nuclease were added to permeabilized cells prepared as described above to remove endogenous RNA. After incubation at room temperature for 12min, 4mM EGTA was then added to terminate the reaction. Membranes were then washed and resuspended in KHM buffer such that the optical density (at 600nm) of 5μL membranes in 500μL KHM buffer was 0.060. These membranes were added to *in vitro* translation reactions containing rabbit reticulocyte lysate (Promega, Flexi), amino acids, KCl, and mRNA encoding HA-Vangl2 or pro/HA-TGFα, which was incubated at 30°C for 60min. Donor membranes were then washed once with B88-LiCl buffer, twice with B88 buffer, and resuspended in B88 buffer.

***In Vitro* Budding Reaction**

Vesicle formation and purification was performed as described previously (Kim et al., 2005), with slight modifications. In detail, donor membranes were incubated where

indicated with rat liver cytosol, recombinant COPII proteins, ATP regeneration system, 0.3mM GTP, and Sar1A H79G. The reaction was carried out at 30°C for 1h, and terminated by incubation on ice for 5min. Donor membranes were removed by centrifugation at 14,000 *g* for 12min at 4°C. The resulting supernatant solution was centrifuged at 115,000 *g* for 25min at 4°C to collect COPII vesicles. Vesicle pellets were then resuspended in 15μL of Buffer C and Laemmli sample buffer. Vesicle samples and original donor membrane samples were resolved by SDS-PAGE, transferred on to PVDF membranes, and subjected to immunoblotting to detect various ER resident proteins and COPII cargo proteins.

COPII Recruitment Assay

The membrane recruitment of COPII components using recombinant Sar1A-GTP-restricted mutant was performed as previously described (Aridor et al., 1995), with modifications. In detail, donor membranes were mixed where indicated with rat liver cytosol, recombinant COPII components, ATP regeneration system, 1mM GTP, and/or 3μg GST-Sar1A-GTP-restricted mutant in a total volume of 100μL. The mixture was incubated at 30°C for 30min, and the reaction was terminated by transfer to ice. Membranes were collected by centrifugation at 20,000 *g* for 10min at 4°C. Supernatant fractions were discarded, and membranes were dissolved by incubation with 1mL of solubilization buffer on ice for 30min, with occasional mixing. Insoluble material was removed by centrifugation at 163,000 *g* for 30min at 4°C. The resulting supernatant solutrion was then incubated with glutathione agarose beads (Pierce) at 4°C for 30min with rotational rocking. Subsequently, the beads were collected by centrifugation and washed three times with solubilization buffer. Beads were eluted by heating in Laemmli sample buffer at 55°C for 15min. Samples were resolved by SDS-PAGE, transferred on to PVDF membranes, and subjected to immunoblotting to detect various ER resident proteins, COPII cargo proteins, and Sec23A.

Purification of Recombinant Proteins

Purification of human Sar1A WT & H79G was performed as described (Kim et al., 2005). Purification of human GST-Sar1A-GTP-restricted form was performed as described (Kim et al., 2005), with modification. Briefly, instead of thrombin cleavage, the GST-tagged recombinant protein was directly eluted with 5mM glutathione in PBS buffer, dialyzed overnight in HKM-G buffer, aliquoted, flash frozen in liquid N_2, and stored at -80°C. Purification of human FLAG-Sec23A/His-Sec24D was performed according to previously described procedures (Kim et al., 2005).

Cytosol Fractionation

To make 100% solution, ammonium sulfate was dissolved in de-ionized water to saturation and the pH was adjusted to 7.2 by addition of KOH. The solution was then filtered and stored at 4°C. Appropriate amounts of 100% ammonium sulfate solution were added to rat liver cytosol to obtain desired final salt concentration. Mixture was incubated on ice for 15min, and then centrifuged at 20,817 *g* for 15min at 4°C to separate pellet and supernatant fractions.

For isoelectric precipitation, 25% ammonium sulfate pellets were resuspended in appropriate buffers (10mM potassium acetate [KOAc], 10% glycerol, pH 4.5, 5.0, or 5.5),

and dialyzed against the same buffer at 4°C overnight. Samples were then subject to centrifugation at 20,817 *g* for 15min at 4°C to remove precipitants.\

All chromatography steps except for the ceramic hydroxyapatite column were carried out using automatic fast protein liquid chromatography (FPLC) stations (ÄKTAFPLC & ÄKTA pure, from GE Healthcare Life Sciences). 25% ammonium sulfate pellets were resuspended in appropriate buffers, buffer exchanged into the same buffers using illustra NAP-5 columns (GE Healthcare Life Sciences), and then loaded onto the column. 1mL pre-packed HiTRAP Q FF, HiTRAP SP FF, and HiTRAP Heparin HP columns were used with the automatic FPLC stations. Macro-Prep ceramic hydroxyapatite type I (Biorad) resin was manually packed into 1mL column for manual fractionation. The respective binding buffers and elution conditions are listed in Table 3.2.

All protein fractions were buffer exchanged into B88 buffer (20mM HEPES, 250mM Sorbitol, 150mM KOAc, 5mM magnesium acetate [$Mg(OAc)_2$], pH 7.2) using Zeba spin desalting columns (Thermo Scientific) prior to addition to *in vitro* budding reactions.

Results

Syntenin-1 Interacts via Its PDZ Domains with proTGFα

Syntenin-1 (Syn1) was identified as a cytosolic protein that specifically interacted with the wild type (WT) form of the C-terminal (CT) cytoplasmic tail of proTGFα in a yeast two-hybrid screen (Fernández-Larrea et al., 1999). The interaction was dependent on the C-terminal valine of proTGFα. Syntenin has two tandem PDZ domains, which both can bind to the C-terminal PDZ binding motifs (PBMs) of interaction partners (Grembecka et al., 2006). Previous studies have identified two key glycine residues, G126 & G210, in the PDZ domains of Syn1 that were critical for binding (Koroll et al., 2001; Wawrzyniak et al., 2012). To determine whether and which PDZ domain is required for its interaction with proTGFα, I cloned Syn1 WT, G126E, G210D, and G126E/G210D into pGAD and tested their interaction with proTGFα CT in a yeast two-hybrid assay.

As shown in Fig. 3.2, a single point mutation G210D completely abolished Syn1 interaction with proTGFα CT, while G126E reduced the strength of interaction. This shows that the second PDZ domain of Syn1 is more important for this interaction with a possible cooperation between the two PDZ domains.

Syntenin-1 Does Not Function in ER Export of proTGFα

Next I tested whether Syn1 plays a role in proTGFα trafficking using the *in vitro* budding reaction. GST-tagged human Syn1 wild type (WT) was purified from *E. coli* with or without the GST-tag. GST-tagged Syn1 G126E G210D was also purified from *E. coli* and the GST-tag was removed by thrombin cleavage (Fig. 3.3A). The recombinant proteins were included in *in vitro* budding reactions and their effects on proTGFα packaging into COPII vesicles were measured.

Addition of GST-Syn1 to *in vitro* budding reactions inhibited rather than stimulated proTGFα budding (Fig. 3.3B). This slight inhibition seemed to be specific to proTGFα, as budding of Sec22, a control cargo, was not affected. As controls, addition of equal amounts of purified GST did not affect budding.

To rule out the possibility that the GST-tag on Syn1 had an adverse effect on budding, Syn1 WT & G126E/G210D mutant were purified and the GST-tag was removed by thrombin cleavage. Syn1 G126E/G210D harbors two point mutations in the PDZ domain that renders the protein unable to bind to proTGFα CT (see Fig. 3.2). Addition of Syn1 WT to the *in vitro* budding reaction again seemed to slightly reduce the efficiency of proTGFα budding (Fig. 3.3C), and this effect seemed again to be limited to proTGFα, as Sec22 budding was not affected. The inhibitory effect on proTGFα budding was not observed when Syn1 G126E/G210D was supplemented to the reaction, presumably due to the inability of the protein to interact with proTGFα.

When rat liver cytosol was immunoblotted for presence of Syn1, none or only trace levels of Syn1 was detected using three different antibodies raised against Syn1 (Fig. 3.3E-F). The difficulty in detecting Syn1 in rat liver cytosol was unexpected, as the budding efficiency of proTGFα after *in vitro* translation using HeLa membranes is quite high, ~5-10% when rat liver cytosol is included at 2mg mL^{-1} final concentration. The extremely low levels, if any, of Syn1 in rat liver cytosol therefore argues against a role for Syn1 in the ER export of proTGFα.

C-Terminus of proTGFα Does Not Specifically Inhibit proTGFα Budding *In Vitro*

To identify cytosolic factor(s) involved in the ER export of proTGFα, again I sought to make use of the cytoplasmic C-terminus of proTGFα. Addition of the wild type C-terminal peptide to the budding reaction may titrate the putative cytosolic factor(s) and inhibit the budding of full-length proTGFα. If the competition were specific, mutant C-terminus deficient for binding would not compete with full-length proTGFα and therefore not affect its COPII packaging.

GST-tagged proTGFα CT wild type (WT) and V160 deletion (ΔV) was purified from *E. coli* (Fig. 3.4A). Curiously, when supplemented in *in vitro* budding reactions at equal amounts, GST-proTGFα CT WT showed no inhibition of full length proTGFα, whereas the ΔV mutant displayed specific inhibition of full-length proTGFα (Fig. 3.4B).

The cytoplasmic C-terminus of proTGFα is quite short, only ~32 amino acids in length, whereas the GST-tag is a large tag of over 20 kDa and known to dimerize. The fusion of a short peptide stretch to a large protein tag could have unintended structural consequences. For instance, the presence of the large GST-tag could prevent binding of proTGFα CT to its interaction partners due to steric clash.

To avoid this possibility, I synthesized short peptides corresponding to the last 10-11 amino acids (Table 3.1). When these synthetic peptides were supplemented in the *in vitro* budding reactions, no significant effect on proTGFα budding was observed (Fig. 3.4C).

Palmitoylation Is Not Required for ER Export of proTGFα

The two cysteines C153 & C154 in the C-terminus of proTGFα had been shown to be palmitoylated (Shum et al., 1996). These two cysteines are located in proximity to the PBM (amino acids 157-160). This raised the possibility of the involvement of palmitoylation in the ER export of proTGFα. This also allowed an alternative explanation for the observation that GST-proTGFα CT WT did not inhibit proTGFα budding but ΔV mutant did: Perhaps GST-proTGFα CT WT did bind to its interaction partner, and therefore the palmitoylation sites were rendered inaccessible to the palmitoylation

machinery. Perhaps the GST-proTGFα CT ΔV was defective for binding and therefore the palmitoylation sites were available for modification. The presence of elevated amounts of the CT ΔV fragments may have competed with the *in vitro* translated full length proTGFα for palmitoylation and thus inhibited the budding of the latter.

To test this hypothesis, I generated pro/HA-TGFα C153S/C154S, a mutant form of proTGFα which had been shown to be defective for palmitoylation (Shum et al., 1996), and tested whether this mutation affected proTGFα budding *in vitro*. Mutation of C153 & C154 did not affect proTGFα budding *in vitro*, while the V160G mutation significantly reduced proTGFα budding efficiency (Fig. 3.5). From this observation I concluded that palmitoylation was not required for ER export of proTGFα.

Purified COPII Proteins Cannot Form Vesicles from HeLa Membranes Treated by *In Vitro* Translation

To test whether rat liver cytosol contained auxiliary factors required for ER export of proTGFα, I tested whether purified COPII proteins could support proTGFα budding *in vitro* (Fig. 3.6A&B). Purified COPII proteins could not support efficient proTGFα budding. Supplementing purified COPII proteins with 0.5mg mL^{-1} rat liver cytosol resulted in packaging of proTGFα into COPII vesicles. However, if rat liver cytosol was heated at 100°C for 5min prior to addition, it could no longer support proTGFα budding. Notably, 0.5mg mL^{-1} rat liver cytosol was not able to promote COPII packaging of proTGFα in the absence of purified COPII proteins (Fig. 3.6A). To test whether simply the presence of higher concentration of protein would be able to support proTGFα budding *in vitro*, I supplemented bovine serum albumin (BSA) with purified COPII proteins in an *in vitro* budding reaction at an amount equal to RLC in the previous experiment. As shown in Fig. 3.6B, presence of BSA in the reaction mix did not support proTGFα budding, suggesting there were indeed factors in RLC whose activity was required for proTGFα transport. However, although purified COPII did not support packaging of proTGFα, neither did it support packaging of the control cargos ERGIC53 and Sec22, raising the question whether purified COPII protein could form any vesicles at all.

HeLa membranes were known to support vesicle formation by purified COPII proteins (Chris Fromme, personal communication). However, in all previous *in vitro* budding reactions, pro/HA-TGFα was artificially inserted into HeLa membranes following *in vitro* translation. Such a procedure subjected membranes to prolonged treatment at 30°C prior to the *in vitro* budding reaction, which could potentially damage the membranes. To test if this was the case, I compared HeLa membranes either untreated or treated by *in vitro* translation side by side in the *in vitro* budding reaction. Indeed, HeLa membranes that had undergone *in vitro* translation were unable to support COPII vesicle formation in presence of purified COPII (Fig. 3.6C). Also, of the Sec24 isoforms tested, Sec24D displayed the most activity. (This must be in the samples without prior exposure to the *in vitro* translation incubation.)

Thus the data so far show that the *in vitro* translation procedure renders HeLa membranes incompetent for vesicle formation when incubated with purified recombinant human COPII proteins. Rat liver cytosol likely contains protein factors that can stabilize the membranes, although the factors themselves may not be directly involved in the biogenesis of COPII vesicles.

Auxiliary Cytosolic Factor(s) Required for COPII Packaging of proTGFα

To circumvent *in vitro* translation, I transiently transfected HeLa cells with plasmids expressing pro/HA-TGFα, grown overnight, and permeabilized cells were harvested the next day for use in the *in vitro* budding reaction. These membranes from transiently transfected HeLa cells were used to determine whether purified COPII proteins could support proTGFα packaging into COPII vesicles *in vitro*.

Cytosol prepared from fresh rat livers was sufficient to support packaging of both pro/HA-TGFα and a control cargo ERGIC53 into COPII vesicles in the *in vitro* budding reaction, in absence of purified COPII proteins (Fig. 3.7A, lanes 3 & 4). Cytosol prepared from frozen rat livers (livers were flash-frozen in liquid nitrogen and then subsequently thawed slowly at 4°C), in contrast, was inactive in the budding reaction (Fig. 3.7A, lanes 5 & 6). Purified COPII proteins, however, supported the efficient packaging of ERGIC53, but not pro/HA-TGFα (Fig. 3.7A, lane 7), suggesting the requirement of a cargo-selective cytosolic factor(s) for the packaging of the latter. Supplementing purified COPII components with inactive cytosol could restore the packaging of pro/HA-TGFα into COPII vesicles (Fig. 3.7A, lanes 8-11).

Although cytosol prepared from frozen rat livers displayed minimal budding activity, it still contained significant amounts of the COPII subunits (Fig. 3.7C, lanes 1 & 2). To rule out the possibility that the pro/HA-TGFα-specific packaging activity was due to the residual COPII components, inactive cytosol was precipitated with 30% ammonium sulfate to pellet the remaining COPII, which removed all detectable COPII from the resulting supernatant (Fig. 3.7C, lane 4). Budding reactions supplementing purified COPII with the 30% ammonium sulfate supernatant (30S) fraction showed specific enhancement of pro/HA-TGFα packaging (Fig. 3.7B, compare lanes 3 & 5), demonstrating that the pro/HA-TGFα-specific activity is not attributable to known COPII components, suggesting the existence of an auxiliary cytosolic factor(s) specifically required in the packaging of pro/HA-TGFα.

Further experiments were conducted to confirm that the observed pro/HA-TGFα packaging activity was a COPII-dependent process. The 30S fraction was unable to support packaging of either ERGIC53 or pro/HA-TGFα in the absence of purified COPII (Fig. 3.7D, lane 7). Supplementing purified COPII components with the 30S fraction greatly enhanced pro/HA-TGFα packaging efficiency (Fig. 3.7D, lanes 9-11), and this activity was inhibited when Sar1A H79G, a dominant negative inhibitor of *in vitro* COPII budding, was included in the reaction (Fig. 3.7D, lane 12), thus confirming that the pro/HA-TGFα-specific activity of the 30S fraction was dependent on COPII.

Finally, pro/HA-TGFα V160G was packaged extremely inefficiently into vesicles (Fig. 3.7D, compare lane 15 with lanes 3 & 16). And as expected, supplementing purified COPII with 30S cytosolic fraction resulted in inefficient packaging of pro/HA-TGFα V160G as well (Fig. 3.7D, compare lanes 22 & 23 with lanes 10 & 11), thus demonstrating the physiological relevance of our findings *in vitro*.

Cornichon-1 Functions as a Cargo Receptor for proTGFα

In HeLa cells, Cornichon-1 (CNIH) had been previously identified as an interaction partner with proTGFα in the ER. The interaction was mapped to occur in the ER lumen and required the extracellular EGF-like domain of proTGFα (Castro et al.,

2007). Based on the known function of Erv14p, the yeast homolog of CNIH, as a COPII cargo receptor (Powers and Barlowe, 1998; Powers and Barlowe, 2002), mammalian CNIH was proposed to play a similar role in the ER export of proTGFα, but so far there has been no direct functional evidence. To ask whether CNIH might indeed play such a role, I generated a CNIH knockout (KO) in HeLa cells using CRISPR/Cas9. Seven clones were expanded and analyzed for expression of CNIH (Fig. 3.8A). Genomic sequencing confirmed that clone #3 was a bona fide genomic knockout of CNIH, and all subsequent experiments were performed using this cell line.

I first assessed the effect of CNIH KO on proTGFα trafficking. CNIH KO resulted in diminished budding efficiency of proTGFα, but also resulted in diminished ERGIC53 budding efficiency (Fig. 3.8B, E, & F). However, Vangl2 and Sec22 budding was not affected (Fig. 3.8C, D, G, & H), suggesting that the effects of CNIH KO was specific and did not result in general disruption of ER export. Importantly, CNIH itself was also packaged very efficiently into COPII vesicles (Fig. 3.8C). Together these data indicate a role for CNIH in the ER export of proTGFα.

Cornichon-1 and Cytosol Factor(s) Are Required for proTGFα Recruitment to the Pre-Budding Complex

The apparent involvement of both a transmembrane cargo receptor and a cytosolic factor(s) in the ER export of proTGFα prompted me to further investigate the mechanism of proTGFα recruitment to the pre-budding complex using the COPII recruitment assay.

To confirm that the trafficking defect of pro/HA-TGFα V160G was not a result of defective binding to CNIH, I performed coimmunoprecipitation experiments and demonstrated that pro/HA-TGFα V160G bound as to CNIH as efficiently as wild type (Fig. 3.9A, lanes 7 & 8).

HeLa cells were transiently transfected with plasmids encoding pro/HA-TGFα WT and membranes were harvested the next day for use in the COPII recruitment assay. When the pre-budding complex was assembled using purified Sec23A/24D heterodimer, pro/HA-TGFα was not recruited (Fig. 3.9B, lane 4). Supplementing the 30% ammonium sulfate supernatant fraction (30S) to the reaction resulted in recruitment of pro/HA-TGFα WT to the pre-budding complex, demonstrating the requirement of cytosolic factor(s) in this process (Fig. 3.9B, lane 5). Notably, while pro/HA-TGFα was recruited to the pre-budding complex, Sec22 was not, indicating cargo specificity. HeLa cells were then transiently transfected with plasmids encoding pro/HA-TGFα V160G, and membranes were harvested for use in the COPII recruitment assay. Interestingly, although the V160G mutant was defective for packaging into COPII vesicles, it was still recruited to the pre-budding complex in the presence of purified Sec23A/24D and the 30S fraction (Fig. 3.9C, lane 5). Finally, HeLa CNIH knockout cells were transiently transfected with plasmids encoding pro/HA-TGFα WT and membranes were harvested for use in the COPII recruitment assay. Removal of CNIH from HeLa membranes prevented pro/HA-TGFα WT from being recruited to the pre-budding complex (Fig. 3.9D, lane 5). As a control, the impact of CNIH knockout on Sec22 recruitment was analyzed. While supplementing the 30S fraction to purified Sec23A/24D did not support Sec22 recruitment to the pre-budding complex, supplementing total rat liver cytosol did (Fig. 3.9E, lane 5). This can be explained by the fact that Sec22 specifically interacts with isoforms A & B of Sec24 (Mancias and Goldberg, 2008). Total rat liver cytosol contains all four Sec24 isoforms,

and thus is able to support Sec22 recruitment to the pre-budding complex. In contrast, the 30S fraction does not contain Sec24, and thus Sec22 cannot be recruited to the pre-budding complex because it is not recognized by Sec24D. More importantly, CNIH knockout does not affect Sec22 recruitment to the pre-budding complex, supporting a specific role for CNIH in proTGFα recruitment (Fig. 3.9E, lane 10).

Efforts to Identify Cytosolic Factor(s) by Protein Fractionation

A biochemical approach was adopted to identify the cytosolic factor(s) in rat liver cytosol that specifically enhanced proTGFα budding *in vitro*. Basically, cytosolic protein was fractionated by various chemical or physical properties, and tested for proTGFα budding stimulating activity (henceforth referred to as "activity of interest"). Due to technical and time constraints, the cytosolic factor(s) were not purified to homogeneity but partially purified cytosolic fractions were obtained, confirming that the activity of interest fractionated distinctly from COPII components.

Ammonium Sulfate Precipitation

Ammonium sulfate precipitation is a gentle and largely reversible method of precipitating proteins. It is commonly employed as a first fractionation step to separate proteins from crude, concentrated samples. Rat liver cytosol prepared from frozen livers was subjected to precipitation at different concentrations of ammonium sulfate, and the pellet and supernatant fractions were collected and analyzed for activity of interest in the budding reaction (Fig. 3.10A). When supplemented with purified COPII in the budding reactions at equal protein amounts, generally the pellet fraction displayed much more activity of interest when compared to the supernatant fraction at $(NH_4)_2SO_4$ concentrations of 20% or more. At lower concentrations (< 20%) of $(NH_4)_2SO_4$, the amount of precipitated protein was small and limited the amount of total protein that could be supplemented to the reactions.

The COPII content of the various cytosolic fractions was also analyzed by immunoblotting (Fig. 3.10B). When $(NH_4)_2SO_4$ concentrations were as low as 25%, the majority of COPII components were already mainly in the pellet fraction. In general consideration of protein yield and specific activity, precipitation at 25% $(NH_4)_2SO_4$ was chosen as a starting step for subsequent rounds of fractionation.

Isoelectric Precipitation

Protein solubility decreases significantly when the pH of the solution approaches the protein's isoelectric point (pI). The propensity for protein precipitation also increases at low salt concentrations. At pH 6.5-8.0, no significant protein precipitation was observed, while at pH 6.0 the majority of the activity of interest was precipitated. This precipitation was largely irreversible as it was extremely difficult to resuspend the pellets back into solution. This suggested that the protein(s) responsible for the activity of interest had a pI of about 6. I then tried further lowering the pH of solution to see if I could sediment the other non-specific proteins while retaining the activity of interest in solution.

As shown in Fig. 3.11, although significant amounts of the activity of interest remained in solution with pH as low as 4.5, there was no significant enrichment of the activity of interest (25μg of total protein was supplemented to purified COPII in each

reaction). This could be either due to partial precipitation of the relevant protein factor(s), or due to decreased activity at non-physiological pH. In either case, separation by isoelectric precipitation would not be an effective method for enriching the activity of interest.

Ion Exchange Chromatography

I next turned to ion exchange chromatography to fractionate the cytosolic proteins by electrostatic charge. The activity of interest was significantly decreased when protein concentrations dropped below 10mg mL^{-1} (data not shown). This drop of activity was attributed to protein instability at low concentrations, and glycerol was included in all chromatography buffers at 10% final concentration to increase protein stability.

Various ion exchange columns were tried which resulted in varying degrees of separation (Table 3.2). Of the columns tested, immobilized Heparin showed the best separation (Fig. 3.12). When a 25% ammonium sulfate pellet fraction was resuspended in loading buffer (10mM potassium phosphate, 10% glycerol, pH 6.5), the majority of the activity of interest bound to the heparin column, and was eluted at relatively high concentrations of salt (KCl). Slight enrichment of activity of interest was also observed (Fig. 3.12B). When the COPII content of these fractions was analyzed, they exhibited a distribution distinctly different from that of the activity of interest (Fig. 3.12, compare panels B & C), thus confirming that the activity of interest cannot be attributed to the activity of known COPII components.

Discussion

The small transmembrane protein proTGFα provided a model cargo molecule that was relatively easy to work with, and allowed for detailed biochemical characterization of the cytosolic requirements for ER export using *in vitro* assays. Originally, I sought to utilize the cytoplasmic C-terminus (CT) of proTGFα to identify cytosolic binding partners that are required for COPII packaging. However, addition of purified proTGFα CT to the *in vitro* budding reaction did not result in inhibition of full length proTGFα budding. . Supplementing short synthetic peptides corresponding to the last 11 amino acids of proTGFα CT to the *in vitro* budding reaction did not inhibit full length proTGFα either. These observations suggested that the soluble CT was not binding with any cytosolic factors involved in COPII packaging of proTGFα.

It could be that the interaction between the CT and the factors of interest was weak and transient, and therefore those factors could not be effectively sequestered to have a significant impact of the budding efficiency of full length proTGFα. As the cytoplasmic CT of proTGFα is quite short, only around 40 amino acids in length, the interaction may need to occur in the context of a membrane surface in order to be stabilized and productive. This may also explain why excess soluble proTGFα CT in the reaction did not have a significant impact on full length proTGFα budding.

The inability of proTGFα CT to affect full length proTGFα budding forced me to adopt an alternative approach to determine the cytosolic requirements for proTGFα ER export. I first tested whether purified COPII proteins could support proTGFα budding *in vitro*. Membranes that had undergone *in vitro* translation prior to addition to the *in vitro* budding reaction could not support COPII vesicle formation when incubated with

purified COPII only, while COPII vesicle formation was quite efficient in the presence of sufficient amounts of rat liver cytosol (final concentration 2mg mL^{-1} or above). This observation suggested that pre-treatment with *in vitro* translation procedures damaged the membranes, and that certain factors in the rat liver cytosol could alleviate the damage. In light of this observation, I sought to side step the need for *in vitro* translation by transiently transfecting HeLa cells with plasmids expressing pro/HA-TGFα before harvesting the membranes. Adopting such an approach allowed me to confirm the existence of an auxiliary cytosolic factor(s) required specifically for ER export of proTGFα. In addition to requirements for an auxiliary cytosolic factor for proTGFα transport, I have also identified a role for Cornichon-1 (CNIH) in the ER export of proTGFα. CNIH likely functions as a cargo receptor that assists in the recruitment of proTGFα to the pre-budding complex.

Interestingly, using the *in vitro* assays, I was able to show that proTGFα V160G is recruited to the pre-budding complex, although it was not packaged into COPII vesicles efficiently. This observation has implications for the mechanism of protein sorting and COPII vesicle packaging. The interaction between cargo molecules and the COPII coat is essential for the enrichment of COPII cargo protein at ER exit sites and a prerequisite for efficient packaging into nascent COPII vesicles. However, an unstated assumption is that so long as cargo can interact with the COPII coat, it will be packaged into COPII vesicles. This does not seem to be the case in light of my observations of proTGFα V160G behavior.

The current model of COPII vesicle formation also does not deal with the issue of kinetics. According to the current model, the efficiency of packaging of a given cargo is related to the affinity between the cargo molecule and the COPII coat. As a result, intuitively one would expect efficiently packaged cargo to be more represented in the pre-budding complexes isolated in the COPII recruitment assay. This was not the case. Sec22 and ERGIC53 are two control cargoes that are efficiently packaged into COPII vesicles *in vitro*. While Sec22 was observed in the pre-budding complex at reasonable levels, ERGIC53 was never observed in the isolated pre-budding complexes, despite it being quite efficiently packaged even in the presence of only purified COPII proteins. Unlike Sec22, which specifically interacts with Sec24A & B, ERGIC53 interacts directly with all four Sec24 isoforms (Wendeler et al., 2007). However, in the COPII recruitment assay, ERGIC53 was not observed in the pre-budding complex when purified Sec23A/24D was included in the reaction mix, nor was it seen in the pre-budding complex even in the presence of total rat liver cytosol (data not shown). This is contrary to my expectations.

The pre-budding complex is an intermediate protein complex formed in the process of cargo sorting and COPII vesicle packaging. To enrich the pre-budding complex, I relied on the use of Sar1A H79G mutant with an N-terminal GST-tag (GST-Sar1·GTP). The Sar1A H79G mutant is defective for its GTPase activity, and is constitutively locked in its active conformation, which is thought to “freeze” the pre-budding complex in place and allow for biochemical isolation and analysis. The GTPase activity of Sar1 has been commonly associated with vesicle coat disassembly. However, in a previous study of pre-budding complex disassociation kinetics using yeast proteins, it was found that Sec23/24 disassociation from SNARE proteins did not correlate with the kinetics of Sar1 GTP hydrolysis (Sato and Nakano, 2005). Moreover, the authors found

that the presence of Sec12p could stabilize Sec23/24 interaction with its SNARE cargoes, presumably by facilitating multiple rounds of Sar1 nucleotide exchange. From these observations, it was proposed that multiple rounds of Sar1p GTP hydrolysis could be a mechanism for protein sorting and cargo packaging into nascent COPII vesicles. From these data, it can also be inferred that, at least in the case of yeast proteins, the pre-budding complex is maintained in a highly dynamic manner prior to cargo packaging. By relying on the GTPase defective Sar1 mutant or non-hydrolyzable GTP analogs as in other studies (Aridor et al., 1999; Kuehn et al., 1998), we are artificially blocking the Sar1 GTP hydrolysis cycle which might lead to the formation of significantly fewer pre-budding complexes, thus explaining the extremely low recovery rate of pre-budding complexes seen in this study and previous work. This may also explain why the GTPase defective mutant form of Sar1 is such a potent inhibitor of COPII vesicle formation *in vitro* – in the absence of GTP hydrolysis cycle, pre-budding complexes are formed in much less abundance and cannot be maintained dynamically.

With these limitations in mind, the observation that the trafficking deficient proTGFα V160G can be recruited to the pre-budding complex is still significant. At the very least this observation points out that interaction with the COPII coat in itself is not sufficient to guarantee efficient packaging into COPII vesicles, and implies that there are still some as yet undescribed processes after the initial assembly of the pre-budding complex and before the formation of COPII vesicles. The V160G mutation in proTGFα results in a kinetic delay in TGFα maturation, which may be due to perturbation of the kinetics of pre-budding complex maintenance.

The COPII recruitment assay demonstrates the requirement of both the cytosolic factor(s) and the transmembrane cargo receptor CNIH for efficient recruitment of proTGFα. Interestingly, a recent study in yeast showed that COPII interaction with both Erv14p (the yeast CNIH homolog) and its client protein was required for efficient export (Pagant et al., 2015). Other studies have shown the importance of cargo protein oligomerization for ER export (Doms et al., 1987; Emery et al., 2000; Nufer et al., 2003; Otte and Barlowe, 2002; Sato and Nakano, 2003). Additionally, *in vitro* studies done with yeast proteins have also shown that Sec23/24p interaction with Sec22p is much more stable when Sec22p is in a fusogenic SNARE complex with Bos1p & Sed5p (Sato and Nakano, 2005). These observations imply that single ER export signals are insufficient to maintain stability of pre-budding complexes, whereas cooperation of two or multiple export signals can provide additional stability that ultimately leads to productive cargo packaging.

Figures

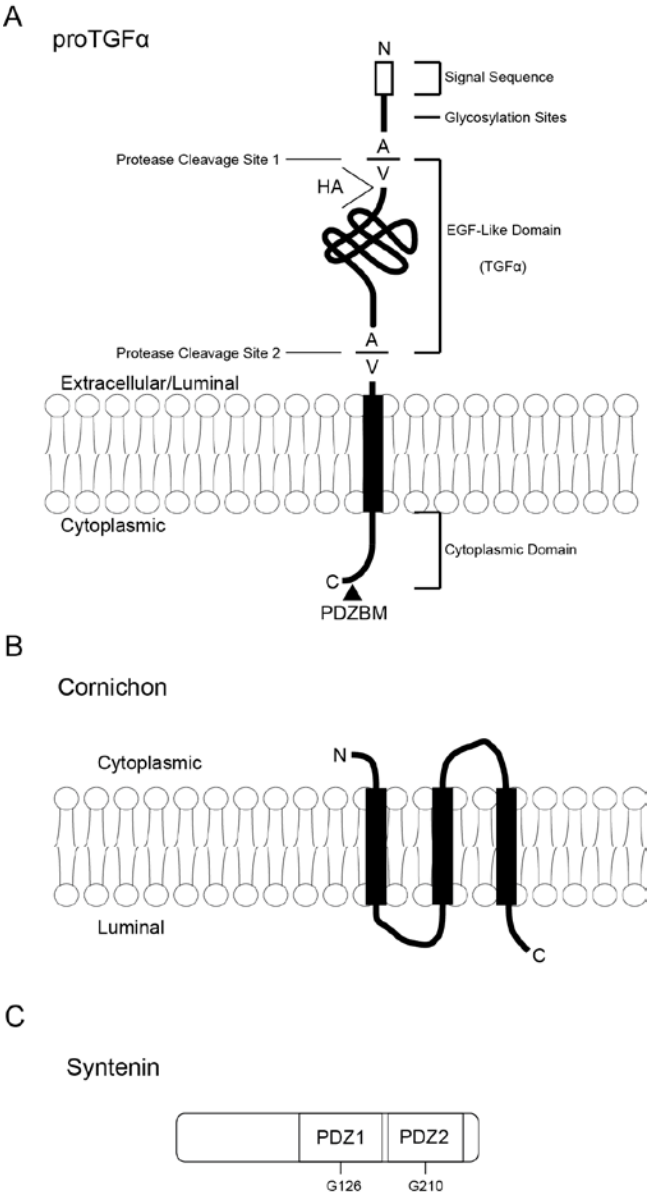

Figure 3.1 – Membrane Topology of proTGFα & Cornichon and Domain Architecture of Syntenin

(A) proTGFα is a single pass transmembrane protein with a short cytoplasmic C-terminus and a signal sequence that is clipped after insertion into the ER. The precursor undergoes successive glycosylation in the ER and Golgi, and at the cell surface it undergoes two successive protease cleavages to release the soluble TGFα into the extracellular space. One HA epitope was inserted right after protease cleavage site 1 for detection in immunoblots, and its position is indicated. The position of the PDZ binding motif (PBM) is also indicated. (B) Cornichon is a three-pass transmembrane protein with a cytoplasmic N-terminus and a luminal C-terminus. (C) Syntenin is a cytosolic protein with two tandem PDZ domains. The key glycine residues in the PDZ domains of human Sytenin-1 are indicated.

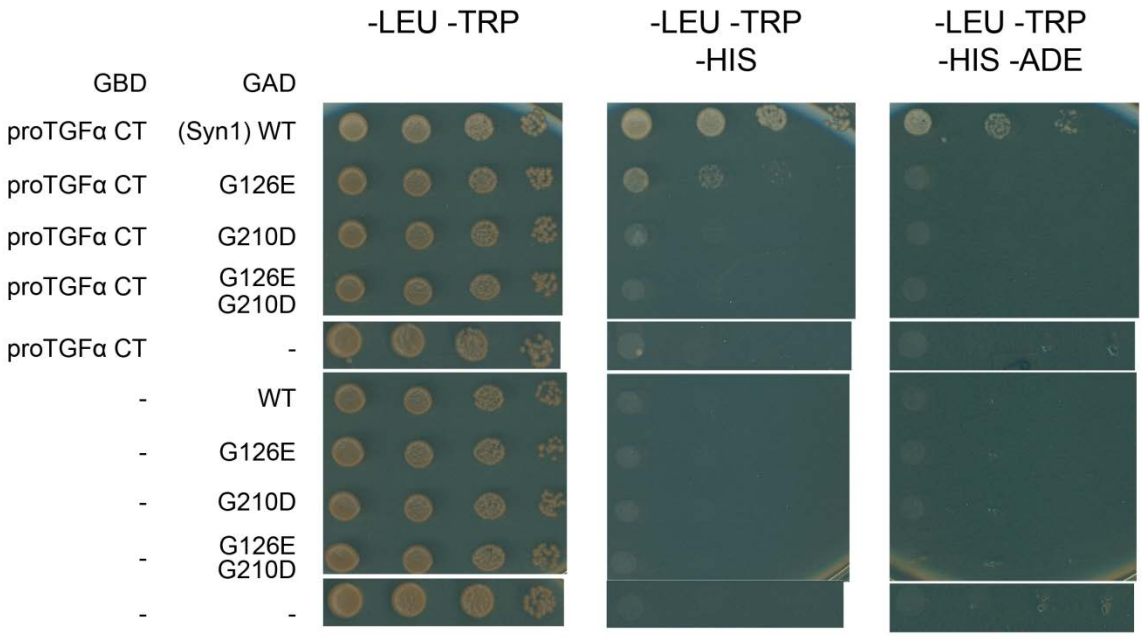

Figure 3.2 – Yeast Two-Hybrid Analysis of Interaction between C-Terminus of proTGFα and Syntenin-1

Yeast two-hybrid analysis of interaction between proTGFα C-terminus (CT) and Syntenin-1 (Syn1). PJ69-4A yeast was co-transformed with two plasmids expressing either Gal4 DNA binding domain (GBD) or Gal4 activating domain (GAD) fused to the indicated protein. Growth on -LEU -TRP -HIS plates indicated weak interaction between the protein combinations, while growth on -LEU -TRP -HIS -ADE plates indicated strong protein interaction. WT: Wild type. G126E: Point mutation that disrupts the first PDZ domain of Syn1. G210D: Point mutation that disrupts the second PDZ domain of Syn1.

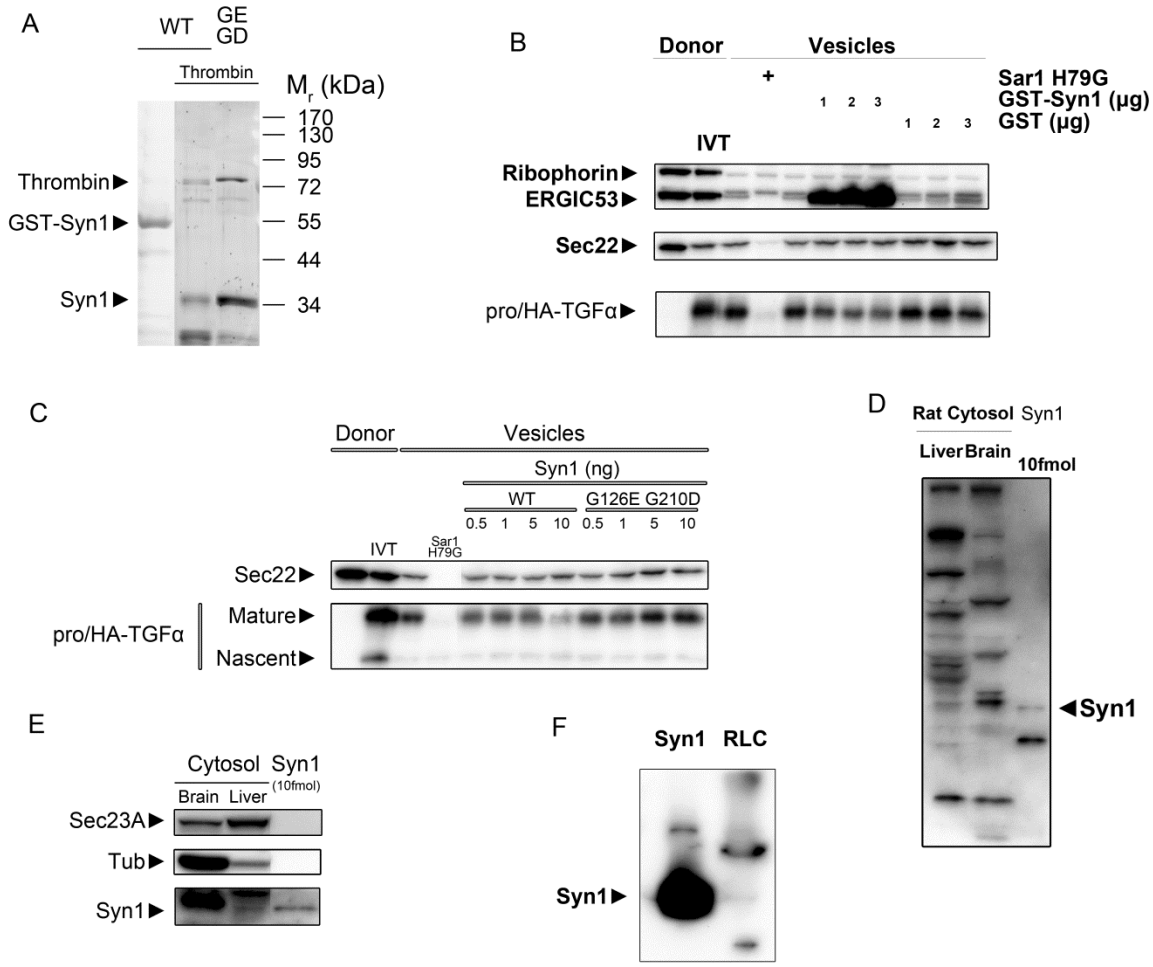

Figure 3.3 – Syn1 Does Not Play a Role in ER Export of proTGFα
(A) Purified Syn1 or GST-Syn1 visualized by SDS-PAGE followed by SYPRO red protein staining. WT: Wild type. GE/GD: G126E/G210D mutant. (B) and (C) *In vitro* budding reaction. pro/HA-TGFα was artificially inserted into HeLa membranes following *in vitro* translation. Reactions were supplemented with the designated amounts of purified recombinant protein as labeled. IVT: *in vitro* translation. Sar1 H79G acts as a dominant negative inhibitor of COPII budding *in vitro*. (D), (E), and (F) Syn1 is present in rat liver cytosol in nearly undetectable levels. Rat liver cytosol, purified recombinant Syn1, and where indicated, rat brain cytosol, were separated by SDS-PAGE and subjected to immunoblotting using three different Syn1 antibodies.

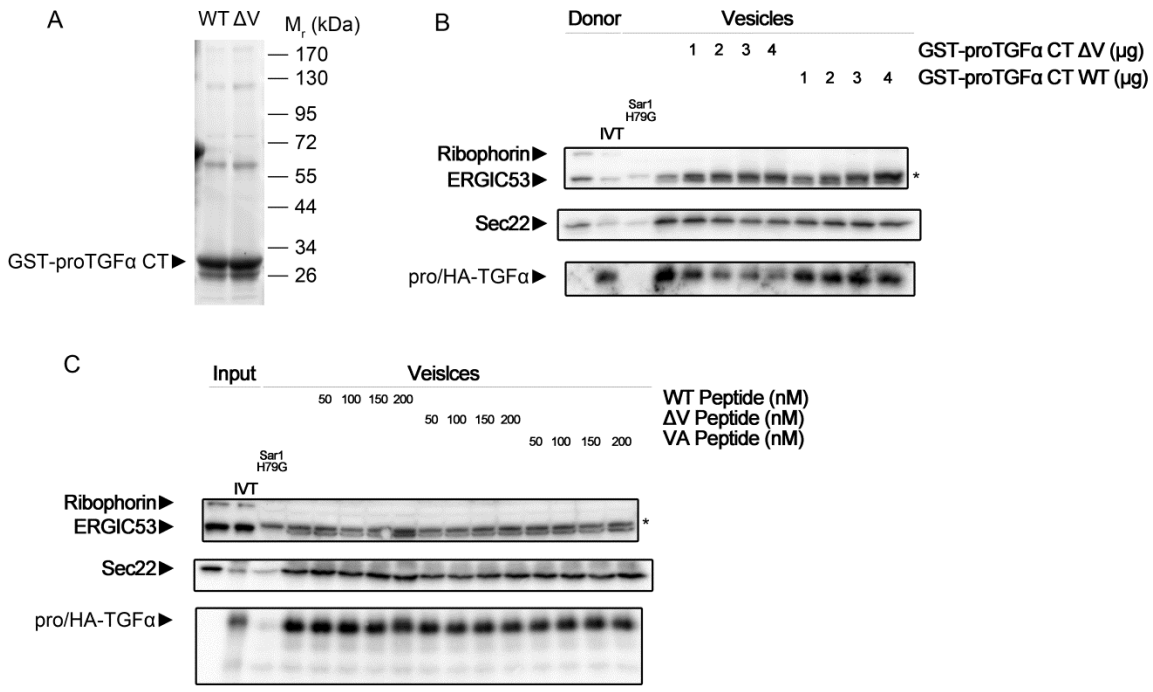

Figure 3.4 – C-Terminus of proTGFα does not Inhibit Budding of Full-Length proTGFα *In Vitro*

(A) Purified GST-tagged proTGFα C-terminus (CT). Samples were separated by SDS-PAGE and stained with SYPRO Red protein stain. WT: Wild type. ΔV: The terminal valine of proTGFα CT was removed. (B) and (C) *In vitro* budding reactions. pro/HA-TGFα was artificially inserted into HeLa membranes following *in vitro* translation, and all budding reactions were performed in the presence of 2mg mL^{-1} rat liver cytosol. The designated amounts of GST-proTGFα CT or synthetic peptides were supplemented to the reaction as indicated. IVT: *In vitro* translation. Sar1 H79G acts as a dominant negative inhibitor of COPII budding *in vitro*. Asterisk: Non-specific band. The bona fide ERGIC53 signal is slightly below the non-specific band and is absent in the presence of Sar1 H79G.

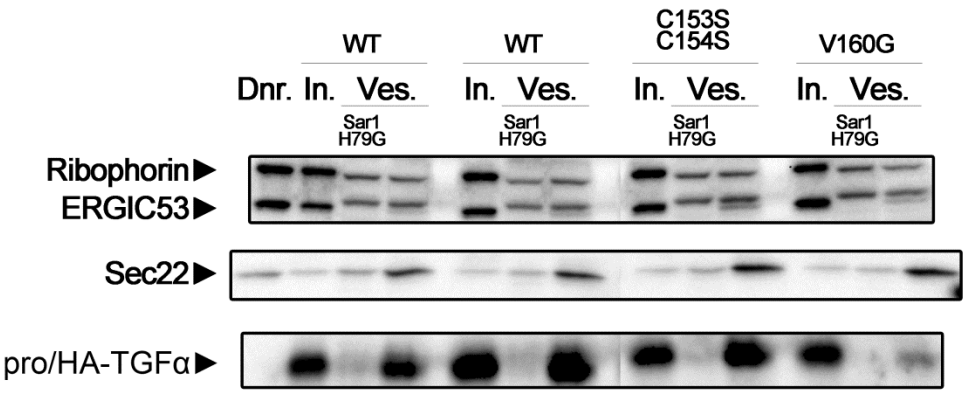

Figure 3.5 – Palmitoylation Is Not Required for ER Export of proTGFα
The palmitoylation deficient C153S/C154S mutant form of proTGFα is packaged efficiently into COPII vesicles *in vitro*. Dnr: Donor membranes, without *in vitro* translation. In: Input membranes, after *in vitro* translation. Ves: Vesicle fractions.

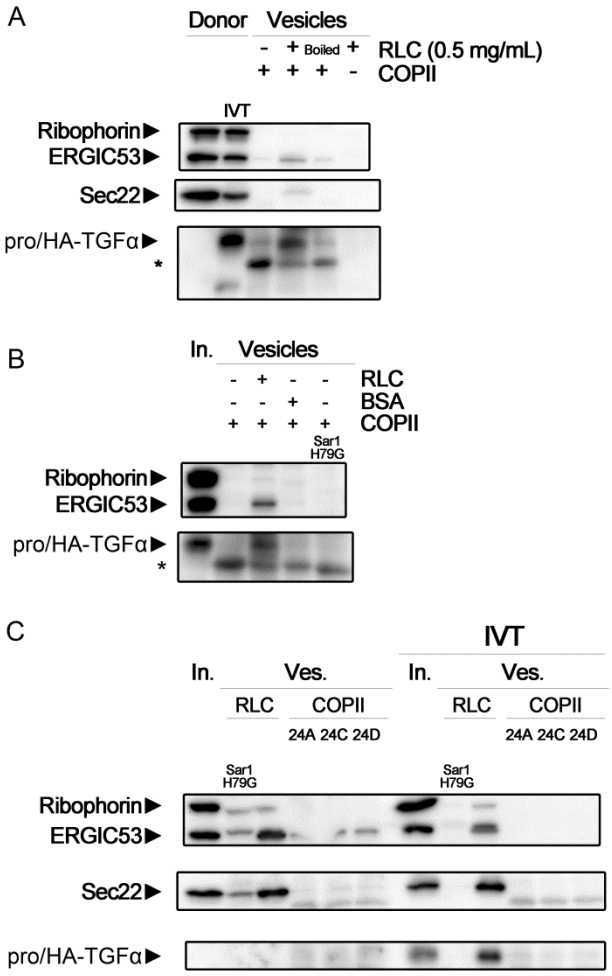

Figure 3.6 – Membranes Treated by In Vitro Translation are Deficient for COPII Vesicle Formation by Purified COPII Proteins

(A) Supplementing purified COPII proteins with limiting amounts of RLC (0.5mg mL^{-1} final concentration) supports proTGFα budding. (B) Supplementing purified COPII proteins with bovine serum albumin (BSA) in equal amount to RLC does not support proTGFα budding. (C) COPII vesicle formation was tested using HeLa membranes, either untreated or treated by *in vitro* translation protocol, in the presence of either rat liver cytosol (RLC) or purified COPII proteins (COPII). IVT: *In vitro* translation. Asterisk: Non-specific protein species. Sar1 H79G acts as a dominant negative inhibitor of COPII budding *in vitro*.

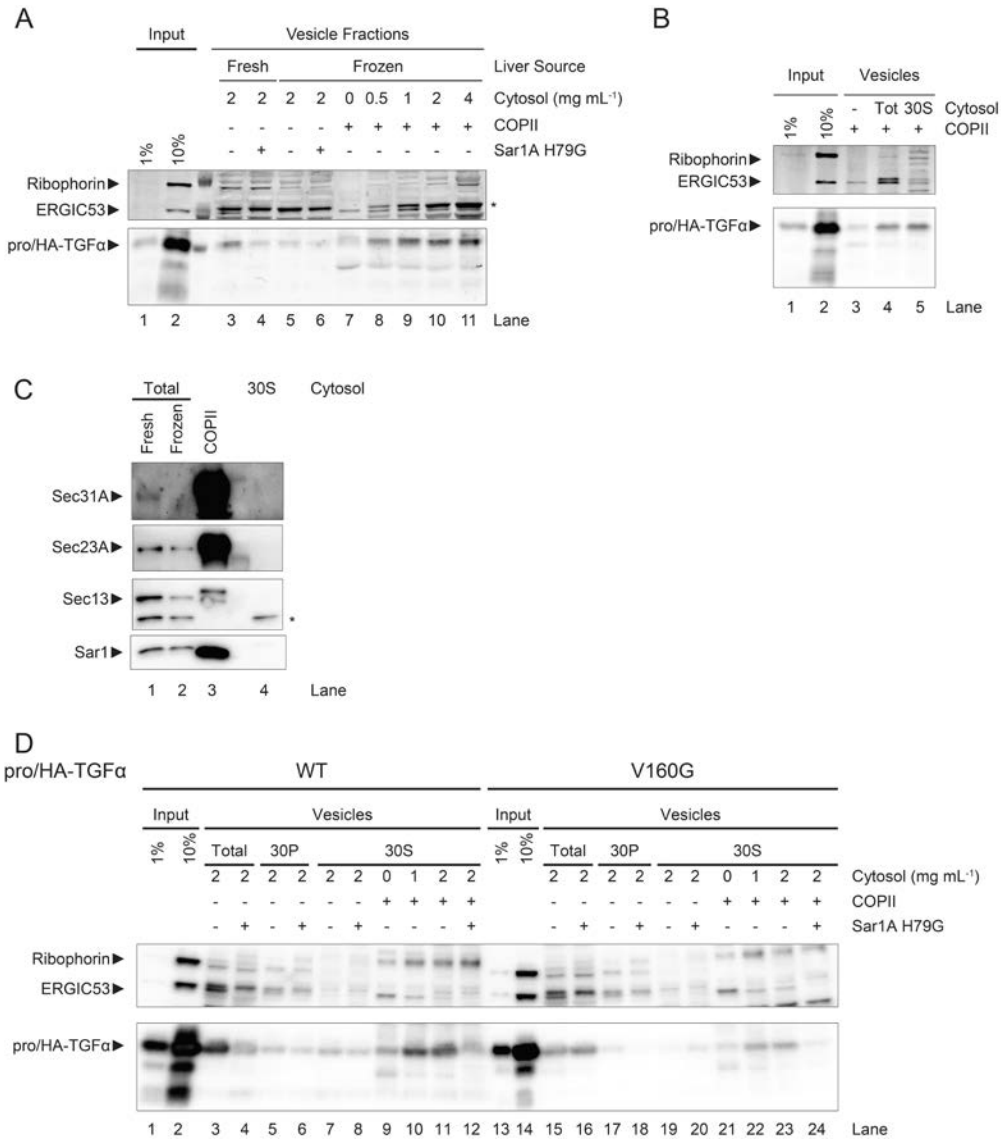

Figure 3.7 – Auxiliary Cytosolic Factor(s) Required for Efficient COPII Packaging of proTGFα

HeLa cells were transfected with plasmids expressing pro/HA-TGFα and membranes were harvested the next day for use in *in vitro* budding reactions. (A) and (B) LiCor scans of *in vitro* budding reactions. Rat liver cytosol was prepared from fresh or frozen rat livers as indicated. (C) Immunoblot of various cytosol fractions and purified COPII samples. Asterisk: Non-specific band. (D) Immunoblot of *in vitro* budding reaction. Tot: Total cytosol extract. 30P: Pellet fraction of cytosol after 30% ammonium sulfate precipitation. 30S: Supernatant fraction of cytosol after 30% ammonium sulfate precipitation. Asterisk: Non-specific band.

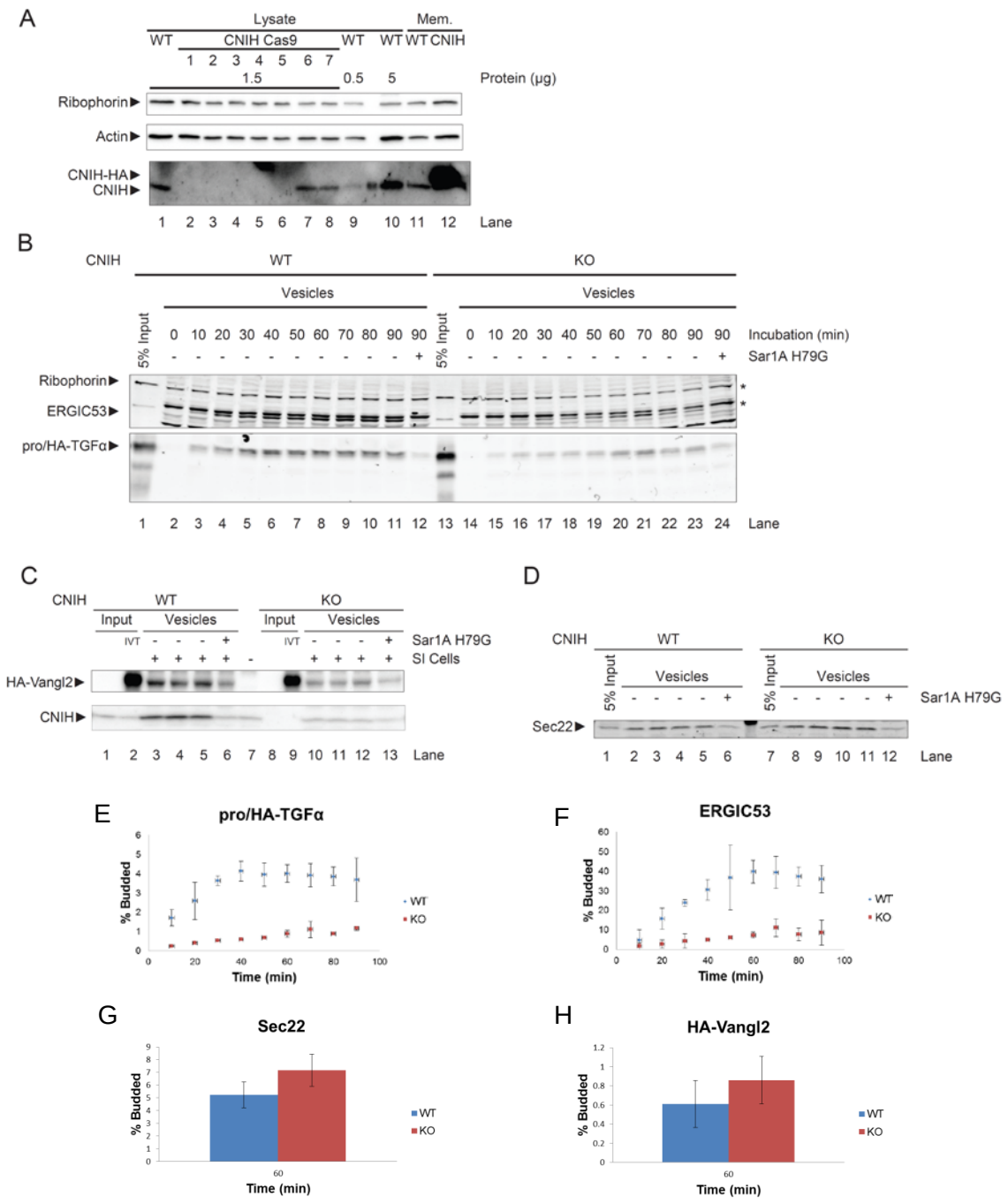

Figure 3.8 – Cornichon-1 Functions in the ER Export of proTGFα
Loss of Cornichon-1 specifically impairs ER export of proTGFα. (A) Immunoblot of HeLa cell lysates (lanes 1-10) or membranes (lanes 11 & 12). WT: Wild type. CNIH: HeLa cells were transiently transfected with a plasmid expressing CNIH-HA. CNIH Cas9: HeLa cells were transiently transfected with plasmids expressing Cas9 and sgRNA targeting the human CNIH gene. (B) LiCor scan of an *in vitro* budding reaction. (C) Immunoblot of an *in vitro* budding reaction. (D) LiCor scan of an *in vitro* budding reaction. (E) – (F) Quantifications of the budding efficiency of pro/HA-TGFα (E), ERGIC53 (F), Sec22 (G), and HA-Vangl2 (H). WT: Wild type. KO: CNIH knockout.

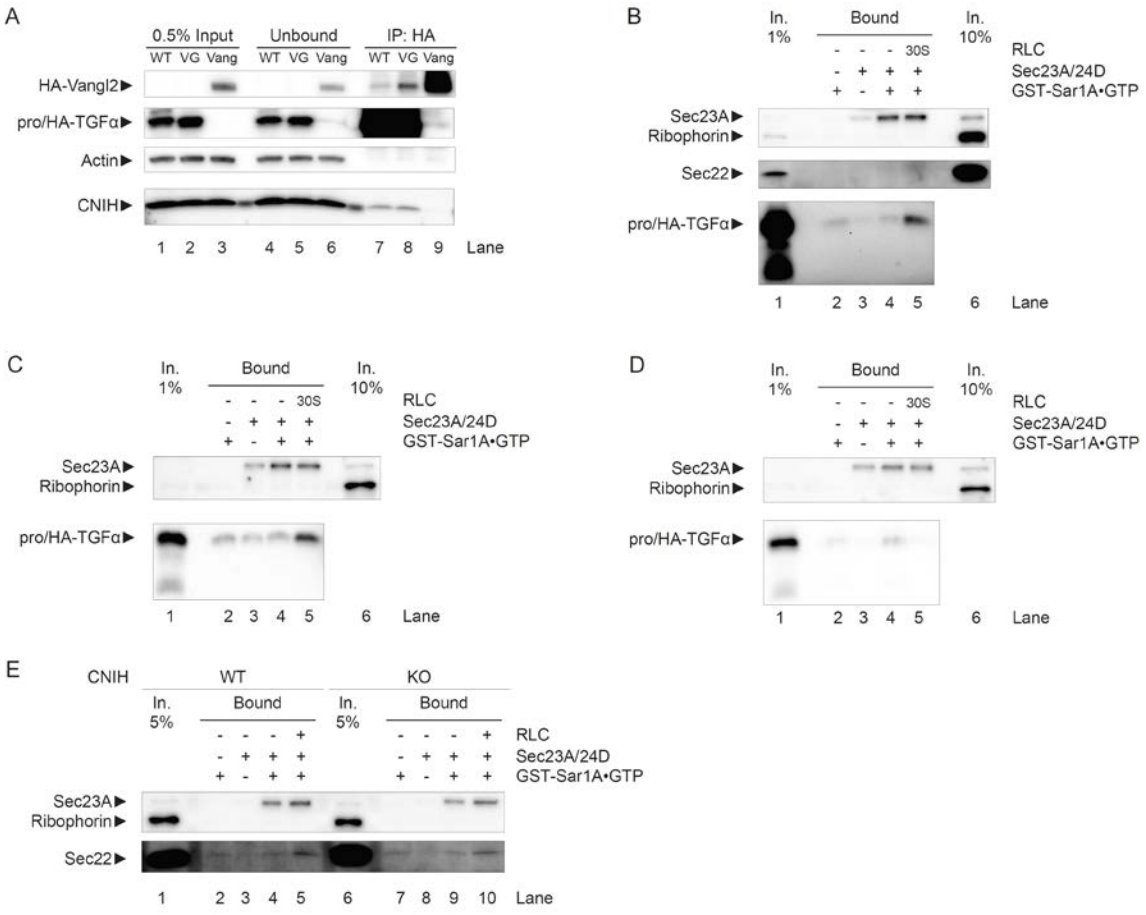

Figure 3.9 – Recruitment of proTGFα to the Pre-Budding Complex Requires Both Cornichon-1 and Cytosolic Factor(s)

(A) Immunoblot of a co-immunoprecipitation experiment. HeLa cells were transfected with plasmids expressing either pro/HA-TGFα wild type (WT), V160G (VG), or HA-Vangl2 (Vang). Cells were then lysed, and proteins were immunoprecipitated with antibodies against the HA epitope. (B) – (E) Immunoblots of COPII recruitment assays. (B) HeLa cells were transiently transfected with plasmids encoding pro/HA-TGFα WT and membranes were harvested for use in the COPII recruitment assay. (C) HeLa cells were transiently transfected with plasmids encoding pro/HA-TGFα V160G and membranes were harvested the next day for use in the COPII recruitment assay. (D) HeLa CNIH knockout cells were transiently transfected with plasmids encoding pro/HA-TGFα and membranes were harvested the next day for use in the COPII recruitment assay. (E) CNIH knockout does not affect Sec22 recruitment to pre-budding complex. RLC: Rat liver cytosol. 30S: 30% supernatant fraction. KO: knock out. GST-Sar1A·GTP: Human Sar1A H79G with an N-terminal GST-tag.

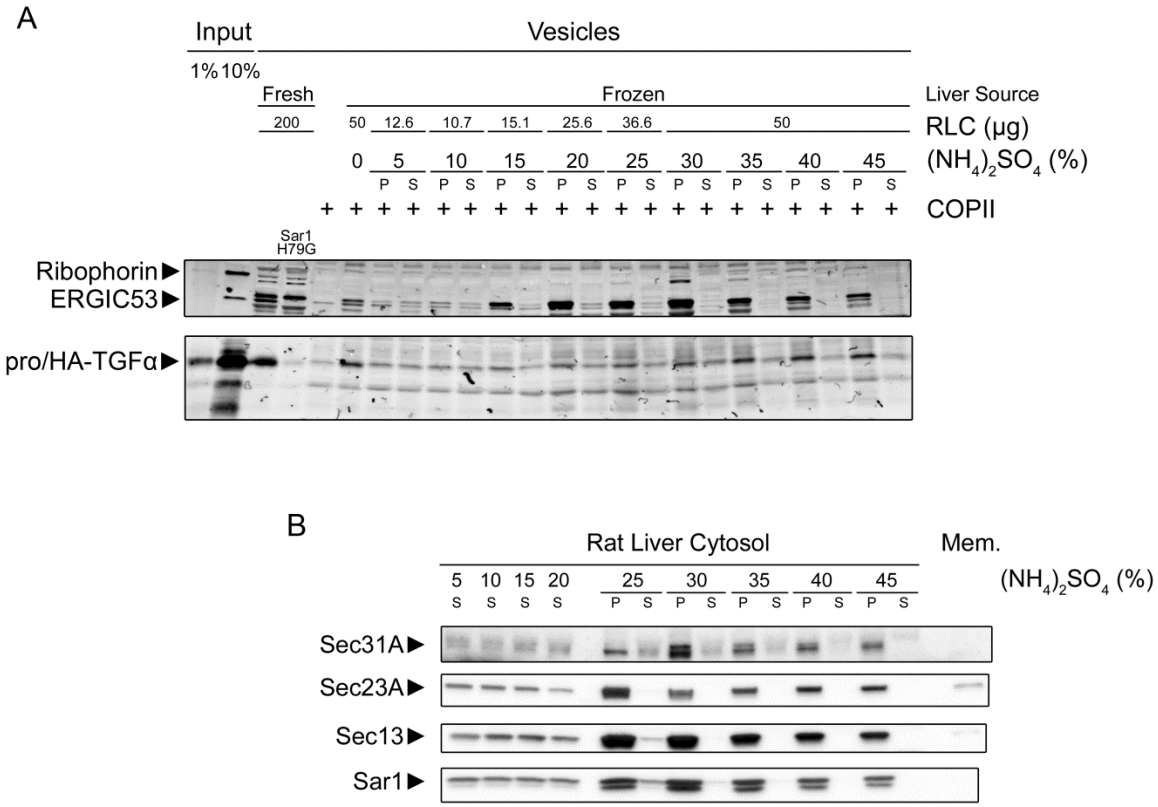

Figure 3.10 – Fractionation of Rat Liver Cytosol by Ammonium Sulfate Precipitation

Rat liver cytosol (RLC) was prepared from frozen rat livers and subjected to ammonium sulfate precipitation at indicated concentrations of $(NH_4)_2SO_4$. (A) Both the pellet (P) and supernatant (S) fractions were tested for activity of interest using the *in vitro* budding reaction. Indicated protein fractions were supplemented at indicated amounts to purified COPII proteins in the *in vitro* budding reaction, and reactions were analyzed by SDS-PAGE followed by LiCOR scanning. (B) Immunoblot analysis of the COPII content of indicated cytosol fractions. 10µg of total protein was loaded in each lane. Mem.: HeLa membranes.

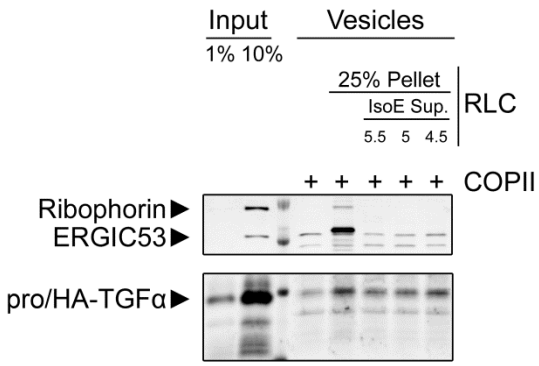

Figure 3.11 – Fractionation of Rat Liver Cytosol by Isoelectric Precipitation Following Ammonium Sulfate Precipitation
The 25% $(NH_4)_2SO_4$ pellet fraction was resuspended in potassium acetate buffers of indicated pH buffer exchanged the same buffer using desalting columns. Insoluble material was removed by centrifugation and the supernatant fraction was collected, buffer exchanged into B88 buffer, and supplemented to purified COPII proteins in the *in vitro* budding reaction. Reactions were then analyzed by SDS-PAGE followed by LiCOR scanning. IsoE Sup.: Isoelectric precipitation supernatant.

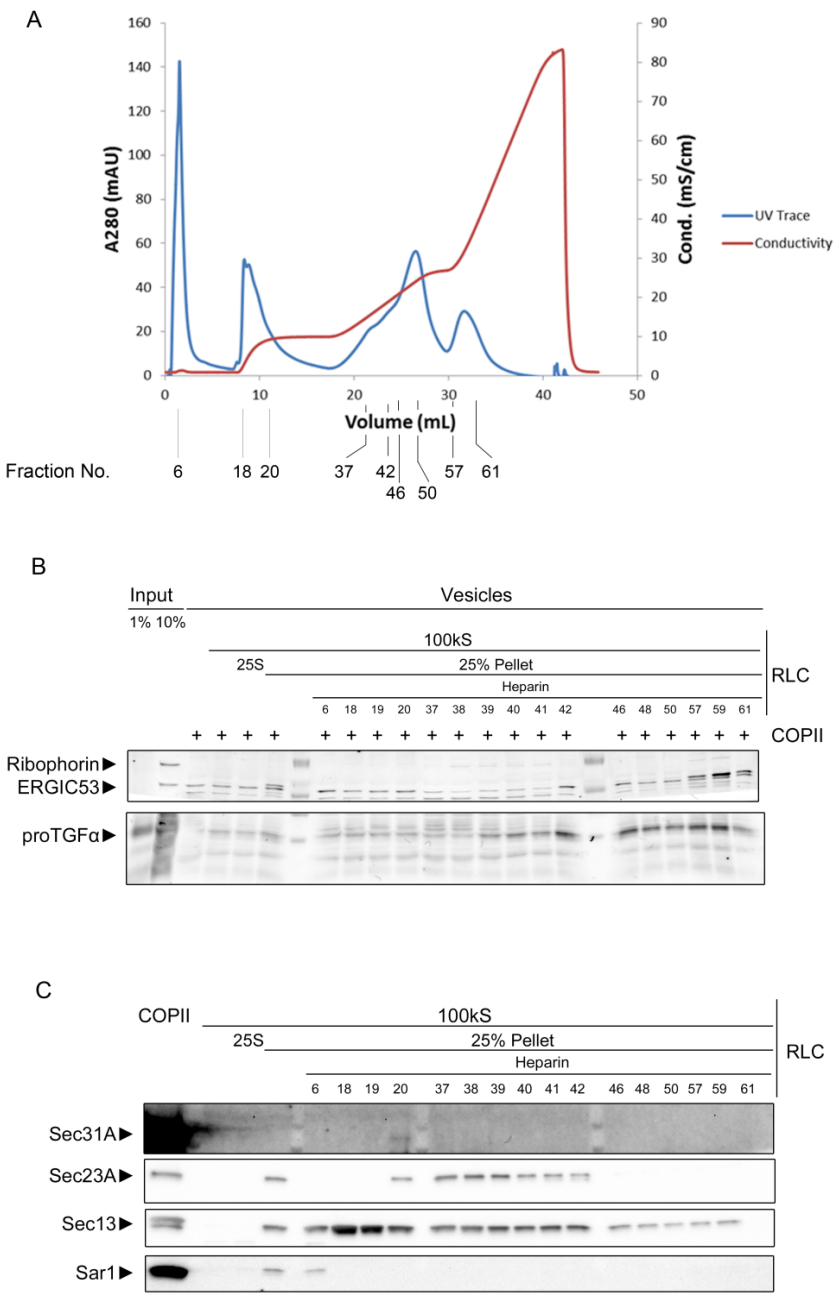

Figure 3.12 – Fractionation of Rat Liver Cytosol by Heparin Chromatography Following Ammonium Sulfate Precipitation

The 25% $(NH_4)_2SO_4$ pellet fraction was resuspended and buffer exchanged into loading buffer (see Table 3.2). Fractionation was performed using FPLC system from GE Health Care and proteins were eluted with up to 1M KCl. (A) Chromatogram of fractionation. Indicated fractions were collected, buffer exchanged into B88 buffer, and further tested for activity of interest and COPII content. (B) Indicated Heparin fractions were supplemented with purified COPII to *in vitro* budding reactions. Reactions were analyzed by SDS-PAGE followed by LiCOR scanning. (C) Indicated Heparin fractions were immunoblotted to analyze COPII content.

Tables

Table 3.1 – Sequence of Synthetic Peptides

Name	Sequence	Molecular Weight (kDa)
WT	RTACCHSETVV	1.21
VA	RTACCHSETVA	1.18
ΔV	RTACCHSETV	1.11

Table 3.2 – Summary of Cytosol Fractionation by Ion Exchange Chromatography

Binding Condition	Q Sepharose	SP Sepharose	Heparin	Ceramic Hydroxyapatite
20mM Tris, 10% Glycerol, pH 7.20	FT, slighty enriched	-	-	-
20mM Tris, 10% Glycerol, pH 8.00	FT & Bound	-	-	-
10mM Potassium phosphate, 10% Glycerol, pH 6.50	-	-	Mostly Bound	-
50mM Potassium phosphate, 10% Glycerol, pH 6.50	-	FT(slightly enriched) & Bound	-	-
10mM Potassium phosphate, 10% Glycerol, pH 8.00	-	-	-	FT (slightly enriched) & Bound

FT: Flow through.
Ceramic hydroxyapatite column was eluted with 500mM potassium phosphate.
The remaining columns were eluted with up to 1M KCl.

Chapter 4: Conclusions and Future Directions

Conclusions

A previous study in the lab had identified the essential role of Sec24B in packaging Vangl2 into COPII vesicles. Finer analysis of Vangl2 trafficking raised the possibility that an additional auxiliary cytosolic factor was involved in addition to the known COPII machinery. The central question of my dissertation is: Are there additional auxiliary cytosolic factor(s) required in the process of COPII vesicle formation?

In Chapter Two, I sought to address this question using Vangl2 as a model cargo molecule. Dishevelled, an interaction partner of Vangl2, was originally postulated to be a possible candidate. This could not be verified as interaction was not observed between Dishevelled and Sec24B. Using Vangl2 as a model cargo molecule was originally appealing because of the two looptail mutants – single amino acid substitutions in the cytoplasmic C-terminus of Vangl2 which resulted in near complete retention of the protein in the ER. The looptail mutants were originally thought to interfere with Vangl2 trafficking by disrupting interaction between Vangl2 and the putative factor(s). However, I found evidence supporting the idea that the looptail mutants result in protein misfolding. Attention was then shifted towards the extreme C-terminus of Vangl2, which harbors a PDZ binding motif (PBM). The terminal valine of Vangl2 had been previously demonstrated to be essential for efficient ER export, and Vangl2 was found to interact with Syntenin-1 (Syn1) via this PBM. However, purified Syn1 was not able to stimulate Vangl2 budding *in vitro*.

Vangl2 is normally localized at the cell surface, whereas overexpression of the protein results in ER retention presumably due to aggregation. To enable analysis of Vangl2 trafficking in the *in vitro* budding reaction, HA-Vangl2 was inserted into membranes following *in vitro* translation. Cos7 membranes were empirically determined to be the most efficient membrane source for Vangl2 insertion. However, purified human COPII proteins were unable to support COPII vesicle formation from Cos7 cells, possibly due to species mismatch (Chris Fromme, personal communication). The low efficiency of Vangl2 budding *in vitro*, and the incompatibility of Cos7 membranes with purified COPII proteins led to a decision to work with an alternative model cargo molecule.

In Chapter Three, I shifted to using proTGFα as a model cargo molecule to address my central question. Originally Syn1 seemed like a likely candidate, but was ruled out after purified Syn1 failed to stimulate proTGFα budding *in vitro*. A C-terminal valine to glycine mutation (V160G) in the very C-terminus of proTGFα resulted in a kinetic delay in proTGFα export from the ER. As this mutation occurs at the very C-terminus of the protein (within the PBM), it is unlikely that it would result in a general structural defect. It is thought that this mutation disrupts interaction between the C-terminus and important cytosolic factor(s), which may explain the defect in trafficking. I then sought to utilize the cytoplasmic C-terminus (CT) of proTGFα to identify the putative cytosolic factor(s) by identifying proteins that preferentially interacted with the wild type (WT) form, but not the V160G mutant. However, addition of purified proTGFα CT WT to the *in vitro* budding reaction did not have any significant effect on the budding efficiency of full length proTGFα. This suggested that the purified soluble CT of proTGFα did not sequester cytosolic factor(s) that were required for proTGFα budding, if

these putative factor(s) existed at all. This observation prompted me to test directly whether purified COPII proteins were sufficient to support proTGFα packaging into COPII vesicles.

Using membranes from HeLa cells transiently transfected with plasmids expressing pro/HA-TGFα, I was able to demonstrate the existence of auxiliary cytosolic factor(s) required for efficient proTGFα packaging into COPII vesicles. Additionally, involvement of Cornichon-1 (CNIH), a transmembrane cargo receptor, was also demonstrated. The efficient recruitment of proTGFα to the pre-budding complex and subsequent packaging into COPII vesicles required the cooperation of both the cytosolic factor(s) and CNIH.

The most interesting observation came when analyzing the recruitment of proTGFα V160G to the pre-budding complex. The trafficking deficient V160G mutant form of proTGFα was recruited to the pre-budding complex, showing that recruitment to the pre-budding complex does not guarantee efficient packaging into COPII vesicles, and suggesting that the packaging of cargo molecules into COPII vesicles may not be as straightforward as previously envisioned.

Vesicular trafficking is a complicated cellular process that involves many distinct steps. Using the COPII recruitment assay and the *in vitro* budding reaction, I have been able to directly analyze two steps in the process of COPII formation: cargo recruitment and vesicle packaging, respectively. This biochemical analysis provided some surprising observations. Cargo recruitment by the COPII coat did not automatically lead to packaging into COPII vesicles, as the current model would suggest. This shows that vesicle packaging is a process that is distinct from cargo recruitment, which provides new insights into how the COPII machinery works.

Future Directions

Cytosol Fractionation

Identification of the cytosolic factor(s) would provide important information and hints to the molecular mechanism by which it influences cargo recruitment and COPII vesicle packaging. Significant effort was invested on this front to fractionate rat liver cytosol and identify the cytosolic factor(s) required for proTGFα trafficking. However, significant technical hurdles limited the success of such an approach.

First of all was the nature of the assay. In classical biochemical fractionation studies, the target protein was usually an enzyme. The assay for measuring the activity of interest was quick and quantitative, which allowed for performing multiple fractionation steps in relatively quick succession and accurate & sensitive measurements of specific activity, a measure of enrichment of the activity of interest. In my work, I primarily relied on the behavior of proTGFα in the *in vitro* budding reaction, which was an immunoblot-based assay that required at least two days before results could be determined. And due to the nature of immunoblots, the sensitivity of the assay was limited.

The second challenge was the properties of the activity of interest. The activity of interest could be kept stable at 4°C for prolonged period of time at high protein concentrations (>10 mg mL^{-1}), but deteriorated rapidly at lower protein concentrations. This, coupled with the long duration of the *in vitro* budding reaction, limited the number of successive fractionation steps that could be taken before the activity of interest

deteriorated. Measures were taken to stabilize protein stability, such as the inclusion of 10% glycerol in all fractionation buffers to stabilize protein folding in solution and the use of desalting columns to minimize the time for buffer exchange. However, despite my best efforts, the stability of the activity of interest could not be enhanced at low protein concentrations.

There are potential methods to overcome these technical challenges. One way is to improve the speed and sensitivity of the *in vitro* budding reaction by employing a luciferase-based assay (Fromme and Kim, 2012). Luciferase could be fused to the luminal domain of proTGFα, and budding efficiency can be gauged by measuring bioluminescence. This would side step the need of immunoblotting and allows the activity of interest to be measured much quicker, and permit performing multiple rounds of fractionation in quick succession. The second way forward would be to increase dramatically the scale of fractionation. For this purpose, it may be desirable to use cytosol prepared from cow or pig livers, which will yield much more starting material for fractionation. Increasing the scale will allow for more successive fractionation steps before protein levels drop below the threshold level (~10 mg mL^{-1}).

Assay Development

Vesicular trafficking is an extremely complex cellular process *in vivo*. Multiple protein machineries generate a plethora of vesicles from different membrane sources. *In vivo* analysis of trafficking in mammalian cells rarely produces clean-cut results, possibly due to the redundancy of the mammalian genome. When significant phenotypes are observed, it is also often very difficult to interpret the exact mechanism due to the complexity of the system.

In vitro biochemical assays provide powerful tools to dissect the molecular function of biomolecules. Especially in the case of vesicular trafficking, biochemical assays allow us to examine more narrowly defined processes. For example, the COPII recruitment assay allowed me to specifically analyze the cargo recruitment process, while the *in vitro* budding reaction permitted me to specifically examine vesicle packaging. These tools proved indispensable in gaining new insights into the process of COPII vesicle formation.

However, despite their considerable strengths, the *in vitro* assays do have significant drawbacks, which may limit their utility in determining the minimal cytosolic requirements for COPII trafficking. Due to low budding efficiency *in vitro*, a significant amount of cargo protein "input" is required in the ER membranes. For cargo proteins that are recycled between the ER and ERGIC, this is not an issue. But for proteins that normally localize at the cell surface, such as Vangl2 and proTGFα, this may present a problem. The issue was initially side-stepped by artificially inserting the proteins into the membranes during *in vitro* translation. However, this damaged the membranes and rendered the membranes incompetent for COPII budding when incubated with purified COPII proteins. And in the case of Vangl2 it was still difficult to obtain a reasonable signal in the vesicle fractions after budding. Overexpression of Vangl2 did result in much more protein localization at the ER, but they were unable to be packaged into COPII vesicles *in vitro*. Overexpression of proTGFα also resulted in much more localization at the ER. Fortunately, the protein at the ER was still competent for budding, although at a reduced efficiency.

The structural stability of transmembrane proteins is usually quite labile, especially for multi-spanning proteins with complex topology. Overexpression of these proteins routinely results in increased ER localization, often attributable to ER retention due to protein misfolding. ER localized proTGFα was still competent for budding likely due to its small size and simple topology. Using overexpression to increase the level of cargo protein in the ER membranes for *in vitro* translation may only be applicable to small, simple cargo proteins such as proTGFα. This technical drawback will significantly limit the utility of the *in vitro* budding reaction in analyzing the molecular requirements for ER export.

An alternative approach could be to utilize the retention using selective hooks (RUSH) system to trap cargo at the ER (Boncompain et al., 2012). The RUSH system consists of an ER resident protein fused to core streptavidin (the hook protein) and the cargo protein of interest fused to streptavidin-binding peptide (SBP). In the absence of biotin, strong interaction between the hook and the SBP on the cargo protein traps the cargo protein at the ER. Addition of biotin releases the interaction and the cargo protein may now leave the ER. While this system was originally developed for *in vivo* characterization of ER to Golgi trafficking, perhaps it could be applied to analyze the molecular requirements of large, complex transmembrane cargo proteins *in vitro*.

Conceptually, one would be able to fuse the small SBP to the transmembrane cargo molecule and trap it in the ER in the absence of biotin. This should allow for abundant amounts of the cargo of interest to accumulate in the ER membranes even at relatively low expression levels. The membranes can then be harvested for use in the *in vitro* budding assay. Then the budding reaction can be performed as usual, but in the presence of biotin to release the cargo from the hook. Of course, efforts will need to be made to find the appropriate ER resident protein to be the hook protein, and to find the appropriate position to insert the SBP on the cargo protein, and additional controls need to be carried out to confirm that insertion of the SBP does not alter normal trafficking.

In my view, combining the RUSH system with the *in vitro* budding reaction may be a simple solution to overcome the limitations of the original assay, and may permit biochemical analysis of a broader range of mammalian cargoes *in vitro*.

References

Adams, E. J., Chen, X.-W. W., O'Shea, K. S. and Ginsburg, D. (2014). Mammalian COPII coat component SEC24C is required for embryonic development in mice. *J. Biol. Chem.* **289**, 20858–70.

Antonny, B., Madden, D., Hamamoto, S., Orci, L. and Schekman, R. (2001). Dynamics of the COPII coat with GTP and stable analogues. *Nat. Cell Biol.* **3**, 531–7.

Antonny, B., Gounon, P., Schekman, R. and Orci, L. (2003). Self-assembly of minimal COPII cages. *EMBO Rep.* **4**, 419–24.

Aridor, M., Bannykh, S. I., Rowe, T. and Balch, W. E. (1995). Sequential coupling between COPII and COPI vesicle coats in endoplasmic reticulum to Golgi transport. *J. Cell Biol.* **131**, 875–93.

Aridor, M., Bannykh, S. I., Rowe, T. and Balch, W. E. (1999). Cargo can modulate COPII vesicle formation from the endoplasmic reticulum. *J. Biol. Chem.* **274**, 4389–99.

Axelrod, J. D., Miller, J. R., Shulman, J. M., Moon, R. T. and Perrimon, N. (1998). Differential recruitment of Dishevelled provides signaling specificity in the planar cell polarity and Wingless signaling pathways. *Genes Dev.* **12**, 2610–22.

Babst, M., Katzmann, D. J., Estepa-Sabal, E. J., Meerloo, T. and Emr, S. D. (2002a). Escrt-III: an endosome-associated heterooligomeric protein complex required for mvb sorting. *Dev. Cell* **3**, 271–82.

Babst, M., Katzmann, D. J., Snyder, W. B., Wendland, B. and Emr, S. D. (2002b). Endosome-associated complex, ESCRT-II, recruits transport machinery for protein sorting at the multivesicular body. *Dev. Cell* **3**, 283–9.

Baines, A. C., Adams, E. J., Zhang, B. and Ginsburg, D. (2013). Disruption of the Sec24d gene results in early embryonic lethality in the mouse. *PLoS ONE* **8**, e61114.

Balch, W. E., Dunphy, W. G., Braell, W. A. and Rothman, J. E. (1984). Reconstitution of the transport of protein between successive compartments of the Golgi measured by the coupled incorporation of N-acetylglucosamine. *Cell* **39**, 405–16.

Barlowe, C. and Schekman, R. (1993). SEC12 encodes a guanine-nucleotide-exchange factor essential for transport vesicle budding from the ER. *Nature* **365**, 347–9.

Bastock, R., Strutt, H. and Strutt, D. (2003). Strabismus is asymmetrically localised and binds to Prickle and Dishevelled during Drosophila planar polarity patterning. *Development* **130**, 3007–3014.

Belden, W. J. and Barlowe, C. (1996). Erv25p, a component of COPII-coated vesicles, forms a complex with Emp24p that is required for efficient endoplasmic reticulum to Golgi transport. *Journal of Biological Chemistry* **271**, 26939–26946.

Bianchi, P., Fermo, E., Vercellati, C., Boschetti, C., Barcellini, W., Iurlo, A., Marcello, A. P., Righetti, P. G. and Zanella, A. (2009). Congenital dyserythropoietic anemia type II (CDAII) is caused by mutations in the SEC23B gene. *Hum. Mutat.* **30**, 1292–8.

Boncompain, G., Divoux, S., Gareil, N., Forges, H. de, Lescure, A., Latreche, L., Mercanti, V., Jollivet, F., Raposo, G. and Perez, F. (2012). Synchronization of secretory protein traffic in populations of cells. *Nat. Methods* **9**, 493–8.

Boyadjiev, S. A., Fromme, J. C., Ben, J., Chong, S. S., Nauta, C., Hur, D. J., Zhang, G., Hamamoto, S., Schekman, R., Ravazzola, M., et al. (2006). Cranio-lenticulo-

sutural dysplasia is caused by a SEC23A mutation leading to abnormal endoplasmic-reticulum-to-Golgi trafficking. *Nat. Genet.* **38**, 1192–7.
Briley, G. P., Hissong, M. A., Chiu, M. L. and Lee, D. C. (1997). The carboxyl-terminal valine residues of proTGF alpha are required for its efficient maturation and intracellular routing. *Mol. Biol. Cell* **8**, 1619–31.
Bryant, N. J. and Stevens, T. H. (1998). Vacuole biogenesis in Saccharomyces cerevisiae: protein transport pathways to the yeast vacuole. *Microbiol. Mol. Biol. Rev.* **62**, 230–47.
Bunker, H. and Snell, G. D. (1948). Linkage of white and waved-1. *The Journal of heredity* **39**, 28.
Bökel, C., Dass, S., Wilsch-Bräuninger, M. and Roth, S. (2006). Drosophila Cornichon acts as cargo receptor for ER export of the TGFalpha-like growth factor Gurken. *Development* **133**, 459–70.
Caro, LG and Palade, GE (1964). Protein synthesis, storage, and discharge in the pancreatic exocrine celL An autoradiographic study. *The Journal of cell biology*.
Castro, C. P., Piscopo, D., Nakagawa, T. and Derynck, R. (2007). Cornichon regulates transport and secretion of TGFalpha-related proteins in metazoan cells. *J. Cell. Sci.* **120**, 2454–66.
Chen, X.-W. W., Wang, H., Bajaj, K., Zhang, P., Meng, Z.-X. X., Ma, D., Bai, Y., Liu, H.-H. H., Adams, E., Baines, A., et al. (2013). SEC24A deficiency lowers plasma cholesterol through reduced PCSK9 secretion. *Elife* **2**, e00444.
Crew, FAE (1933). Waved: an autosomal recessive coat form character in the mouse. *Journal of Genetics* **27**, 95–96.
Curtin, J. A., Quint, E., Tsipouri, V., Arkell, R. M., Cattanach, B., Copp, A. J., Henderson, D. J., Spurr, N., Stanier, P., Fisher, E. M., et al. (2003). Mutation of Celsr1 disrupts planar polarity of inner ear hair cells and causes severe neural tube defects in the mouse. *Curr. Biol.* **13**, 1129–33.
Dacks, J. B. and Field, M. C. (2007). Evolution of the eukaryotic membrane-trafficking system: origin, tempo and mode. *J. Cell. Sci.* **120**, 2977–85.
Derynck, R., Roberts, A. B., Winkler, M. E., Chen, E. Y. and Goeddel, D. V. (1984). Human transforming growth factor-alpha: precursor structure and expression in E. coli. *Cell* **38**, 287–97.
Djiane, A., Riou, J., Umbhauer, M., Boucaut, J. and Shi, D. (2000). Role of frizzled 7 in the regulation of convergent extension movements during gastrulation in Xenopus laevis. *Development* **127**, 3091–100.
Doms, R. W., Keller, D. S., Helenius, A. and Balch, W. E. (1987). Role for adenosine triphosphate in regulating the assembly and transport of vesicular stomatitis virus G protein trimers. *J. Cell Biol.* **105**, 1957–69.
Embley, T. M. and Martin, W. (2006). Eukaryotic evolution, changes and challenges. *Nature* **440**, 623–30.
Emery, G., Rojo, M. and Gruenberg, J. (2000). Coupled transport of p24 family members. *J. Cell. Sci.* **113 (Pt 13)**, 2507–16.
Etheridge, S. L., Ray, S., Li, S., Hamblet, N. S., Lijam, N., Tsang, M., Greer, J., Kardos, N., Wang, J., Sussman, D. J., et al. (2008). Murine dishevelled 3 functions in redundant pathways with dishevelled 1 and 2 in normal cardiac outflow tract, cochlea, and neural tube development. *PLoS Genet.* **4**, e1000259.

Feiguin, F., Hannus, M., Mlodzik, M. and Eaton, S. (2001). The ankyrin repeat protein Diego mediates Frizzled-dependent planar polarization. *Dev. Cell* **1**, 93–101.
Fernández-Larrea, J., Merlos-Suárez, A., Ureña, J. M., Baselga, J. and Arribas, J. (1999). A role for a PDZ protein in the early secretory pathway for the targeting of proTGF-alpha to the cell surface. *Mol. Cell* **3**, 423–33.
Field, M. C. and Dacks, J. B. (2009). First and last ancestors: reconstructing evolution of the endomembrane system with ESCRTs, vesicle coat proteins, and nuclear pore complexes. *Curr. Opin. Cell Biol.* **21**, 4–13.
Fromme, J. C. and Kim, J. (2012). A rapid and quantitative coat protein complex II vesicle formation assay using luciferase reporters. *Anal. Biochem.* **421**, 482–8.
Fromme, J. C., Ravazzola, M., Hamamoto, S., Al-Balwi, M., Eyaid, W., Boyadjiev, S. A., Cosson, P., Schekman, R. and Orci, L. (2007). The genetic basis of a craniofacial disease provides insight into COPII coat assembly. *Dev. Cell* **13**, 623–34.
Gao, C. and Chen, Y.-G. G. (2010). Dishevelled: The hub of Wnt signaling. *Cell. Signal.* **22**, 717–27.
Garbes, L., Kim, K., Rieß, A., Hoyer-Kuhn, H., Beleggia, F., Bevot, A., Kim, M. J., Huh, Y. H., Kweon, H.-S. S., Savarirayan, R., et al. (2015). Mutations in SEC24D, encoding a component of the COPII machinery, cause a syndromic form of osteogenesis imperfecta. *Am. J. Hum. Genet.* **96**, 432–9.
Gietz, R. D. and Schiestl, R. H. (2007). High-efficiency yeast transformation using the LiAc/SS carrier DNA/PEG method. *Nat Protoc* **2**, 31–4.
Green, M. C. (1989). Catalog of mutant genes and polymorphic loci.pp. 8–278. Oxford: Oxford University Press.
Grembecka, J., Cierpicki, T., Devedjiev, Y., Derewenda, U., Kang, B. S., Bushweller, J. H. and Derewenda, Z. S. (2006). The binding of the PDZ tandem of syntenin to target proteins. *Biochemistry* **45**, 3674–83.
Gubb, D. and García-Bellido, A. (1982). A genetic analysis of the determination of cuticular polarity during development in Drosophila melanogaster. *J Embryol Exp Morphol* **68**, 37–57.
Hamblet, N. S., Lijam, N., Ruiz-Lozano, P., Wang, J., Yang, Y., Luo, Z., Mei, L., Chien, K. R., Sussman, D. J. and Wynshaw-Boris, A. (2002). Dishevelled 2 is essential for cardiac outflow tract development, somite segmentation and neural tube closure. *Development* **129**, 5827–38.
Held, L. I., Duarte, C. M. and Derakhshanian, K. (1986). Extra joints and misoriented bristles on Drosophila legs. *Prog. Clin. Biol. Res.* **217A**, 293–6.
Herring, B. E., Shi, Y., Suh, Y. H., Zheng, C.-Y. Y., Blankenship, S. M., Roche, K. W. and Nicoll, R. A. (2013). Cornichon proteins determine the subunit composition of synaptic AMPA receptors. *Neuron* **77**, 1083–96.
Herzig, Y., Sharpe, H. J., Elbaz, Y., Munro, S. and Schuldiner, M. (2012). A systematic approach to pair secretory cargo receptors with their cargo suggests a mechanism for cargo selection by Erv14. *PLoS Biol.* **10**, e1001329.
Hoshino, H., Uchida, T., Otsuki, T., Kawamoto, S., Okubo, K., Takeichi, M. and Chisaka, O. (2007). Cornichon-like protein facilitates secretion of HB-EGF and regulates proper development of cranial nerves. *Mol. Biol. Cell* **18**, 1143–52.

Huang, M., Weissman, J. T., Beraud-Dufour, S., Luan, P., Wang, C., Chen, W., Aridor, M., Wilson, I. A. and Balch, W. E. (2001). Crystal structure of Sar1-GDP at 1.7 A resolution and the role of the NH2 terminus in ER export. *J. Cell Biol.* **155**, 937–48.
Huber, H., Küper, U., Daxer, S. and Rachel, R. (2012). The unusual cell biology of the hyperthermophilic Crenarchaeon Ignicoccus hospitalis. *Antonie Van Leeuwenhoek* **102**, 203–19.
Iliescu, A., Gravel, M., Horth, C., Kibar, Z. and Gros, P. (2011). Loss of membrane targeting of Vangl proteins causes neural tube defects. *Biochemistry* **50**, 795–804.
James, P., Halladay, J. and Craig, E. A. (1996). Genomic libraries and a host strain designed for highly efficient two-hybrid selection in yeast. *Genetics* **144**, 1425–36.
Jensen, D. (2010). COPII Specificity and the Regulation of Anterograde Transport for Planar Cell Polarity Proteins in Neural Tube Development.
Jessen, J. R., Topczewski, J., Bingham, S., Sepich, D. S., Marlow, F., Chandrasekhar, A. and Solnica-Krezel, L. (2002). Zebrafish trilobite identifies new roles for Strabismus in gastrulation and neuronal movements. *Nat. Cell Biol.* **4**, 610–5.
Jones, B., Jones, E. L., Bonney, S. A., Patel, H. N., Mensenkamp, A. R., Eichenbaum-Voline, S., Rudling, M., Myrdal, U., Annesi, G., Naik, S., et al. (2003). Mutations in a Sar1 GTPase of COPII vesicles are associated with lipid absorption disorders. *Nat. Genet.* **34**, 29–31.
Kaiser, C. A. and Schekman, R. (1990). Distinct sets of SEC genes govern transport vesicle formation and fusion early in the secretory pathway. *Cell* **61**, 723–33.
Katzmann, D. J., Babst, M. and Emr, S. D. (2001). Ubiquitin-dependent sorting into the multivesicular body pathway requires the function of a conserved endosomal protein sorting complex, ESCRT-I. *Cell* **106**, 145–55.
Katzmann, D. J., Stefan, C. J., Babst, M. and Emr, S. D. (2003). Vps27 recruits ESCRT machinery to endosomes during MVB sorting. *J. Cell Biol.* **162**, 413–23.
Kibar, Z., Underhill, D. A., Canonne-Hergaux, F., Gauthier, S., Justice, M. J. and Gros, P. (2001a). Identification of a new chemically induced allele (Lp(m1Jus)) at the loop-tail locus: morphology, histology, and genetic mapping. *Genomics* **72**, 331–7.
Kibar, Z., Vogan, K. J., Groulx, N., Justice, M. J., Underhill, D. A. and Gros, P. (2001b). Ltap, a mammalian homolog of Drosophila Strabismus/Van Gogh, is altered in the mouse neural tube mutant Loop-tail. *Nat. Genet.* **28**, 251–5.
Kim, J., Hamamoto, S., Ravazzola, M., Orci, L. and Schekman, R. (2005). Uncoupled packaging of amyloid precursor protein and presenilin 1 into coat protein complex II vesicles. *J. Biol. Chem.* **280**, 7758–68.
Koroll, M., Rathjen, F. G. and Volkmer, H. (2001). The neural cell recognition molecule neurofascin interacts with syntenin-1 but not with syntenin-2, both of which reveal self-associating activity. *J. Biol. Chem.* **276**, 10646–54.
Krasnow, R. E., Wong, L. L. and Adler, P. N. (1995). Dishevelled is a component of the frizzled signaling pathway in Drosophila. *Development* **121**, 4095–102.
Kuehn, M. J., Herrmann, J. M. and Schekman, R. (1998). COPII-cargo interactions direct protein sorting into ER-derived transport vesicles. *Nature* **391**, 187–90.
Kurihara, T., Hamamoto, S., Gimeno, R. E., Kaiser, C. A., Schekman, R. and Yoshihisa, T. (2000). Sec24p and Iss1p function interchangeably in transport vesicle formation from the endoplasmic reticulum in Saccharomyces cerevisiae. *Mol. Biol. Cell* **11**, 983–98.

Lang, M. R., Lapierre, L. A., Frotscher, M., Goldenring, J. R. and Knapik, E. W. (2006). Secretory COPII coat component Sec23a is essential for craniofacial chondrocyte maturation. *Nat. Genet.* **38**, 1198–203.
Larco, J. E. de and Todaro, G. J. (1978). Growth factors from murine sarcoma virus-transformed cells. *Proc. Natl. Acad. Sci. U.S.A.* **75**, 4001–5.
Lei, Y.-P. P., Zhang, T., Li, H., Wu, B.-L. L., Jin, L. and Wang, H.-Y. Y. (2010). VANGL2 mutations in human cranial neural-tube defects. *N. Engl. J. Med.* **362**, 2232–5.
Lijam, N., Paylor, R., McDonald, M. P., Crawley, J. N., Deng, C. X., Herrup, K., Stevens, K. E., Maccaferri, G., McBain, C. J., Sussman, D. J., et al. (1997). Social interaction and sensorimotor gating abnormalities in mice lacking Dvl1. *Cell* **90**, 895–905.
Mancias, J. D. and Goldberg, J. (2008). Structural basis of cargo membrane protein discrimination by the human COPII coat machinery. *EMBO J.* **27**, 2918–28.
Mann, G. B., Fowler, K. J., Gabriel, A., Nice, E. C., Williams, R. L. and Dunn, A. R. (1993). Mice with a null mutation of the TGF alpha gene have abnormal skin architecture, wavy hair, and curly whiskers and often develop corneal inflammation. *Cell* **73**, 249–61.
Merte, J., Jensen, D., Wright, K., Sarsfield, S., Wang, Y., Schekman, R. and Ginty, D. D. (2010). Sec24b selectively sorts Vangl2 to regulate planar cell polarity during neural tube closure. *Nat. Cell Biol.* **12**, 41–6; sup pp 1–8.
Montcouquiol, M., Rachel, R. A., Lanford, P. J., Copeland, N. G., Jenkins, N. A. and Kelley, M. W. (2003). Identification of Vangl2 and Scrb1 as planar polarity genes in mammals. *Nature* **423**, 173–7.
Nakanishi, H., Suda, Y. and Neiman, A. M. (2007). Erv14 family cargo receptors are necessary for ER exit during sporulation in Saccharomyces cerevisiae. *J. Cell. Sci.* **120**, 908–16.
Nevo, R., Charuvi, D., Shimoni, E., Schwarz, R., Kaplan, A., Ohad, I. and Reich, Z. (2007). Thylakoid membrane perforations and connectivity enable intracellular traffic in cyanobacteria. *EMBO J.* **26**, 1467–73.
Novick, P. and Schekman, R. (1979). Secretion and cell-surface growth are blocked in a temperature-sensitive mutant of Saccharomyces cerevisiae. *Proc. Natl. Acad. Sci. U.S.A.* **76**, 1858–62.
Novick, P., Field, C. and Schekman, R. (1980). Identification of 23 complementation groups required for post-translational events in the yeast secretory pathway. *Cell* **21**, 205–15.
Nufer, O., Kappeler, F., Guldbrandsen, S. and Hauri, H.-P. P. (2003). ER export of ERGIC-53 is controlled by cooperation of targeting determinants in all three of its domains. *J. Cell. Sci.* **116**, 4429–40.
Ohisa, S., Inohaya, K., Takano, Y. and Kudo, A. (2010). sec24d encoding a component of COPII is essential for vertebra formation, revealed by the analysis of the medaka mutant, vbi. *Dev. Biol.* **342**, 85–95.
Otte, S. and Barlowe, C. (2002). The Erv41p-Erv46p complex: multiple export signals are required in trans for COPII-dependent transport from the ER. *EMBO J.* **21**, 6095–104.
Pagant, S., Wu, A., Edwards, S., Diehl, F. and Miller, E. A. (2015). Sec24 is a coincidence detector that simultaneously binds two signals to drive ER export. *Curr. Biol.* **25**, 403–12.
Park, M. and Moon, R. T. (2002). The planar cell-polarity gene stbm regulates cell behaviour and cell fate in vertebrate embryos. *Nat. Cell Biol.* **4**, 20–5.

Pearse, B. M. (1976). Clathrin: a unique protein associated with intracellular transfer of membrane by coated vesicles. *Proc. Natl. Acad. Sci. U.S.A.* **73**, 1255–9.
Peng, R., Antoni, A. De and Gallwitz, D. (2000). Evidence for overlapping and distinct functions in protein transport of coat protein Sec24p family members. *J. Biol. Chem.* **275**, 11521–8.
Powers, J. and Barlowe, C. (1998). Transport of axl2p depends on erv14p, an ER-vesicle protein related to the Drosophila cornichon gene product. *J. Cell Biol.* **142**, 1209–22.
Powers, J. and Barlowe, C. (2002). Erv14p directs a transmembrane secretory protein into COPII-coated transport vesicles. *Molecular biology of the cell* **13**, 880–91.
Roberg, K. J., Crotwell, M., Espenshade, P., Gimeno, R. and Kaiser, C. A. (1999). LST1 is a SEC24 homologue used for selective export of the plasma membrane ATPase from the endoplasmic reticulum. *J. Cell Biol.* **145**, 659–72.
Roberts, A. B., Frolik, C. A., Anzano, M. A. and Sporn, M. B. (1983). Transforming growth factors from neoplastic and nonneoplastic tissues. *Fed. Proc.* **42**, 2621–6.
Roth, S., Neuman-Silberberg, F. S., Barcelo, G. and Schüpbach, T. (1995). cornichon and the EGF receptor signaling process are necessary for both anterior-posterior and dorsal-ventral pattern formation in Drosophila. *Cell* **81**, 967–78.
Sarmah, S., Barrallo-Gimeno, A., Melville, D. B., Topczewski, J., Solnica-Krezel, L. and Knapik, E. W. (2010). Sec24D-dependent transport of extracellular matrix proteins is required for zebrafish skeletal morphogenesis. *PLoS ONE* **5**, e10367.
Sato, K. and Nakano, A. (2003). Oligomerization of a cargo receptor directs protein sorting into COPII-coated transport vesicles. *Mol. Biol. Cell* **14**, 3055–63.
Sato, K. and Nakano, A. (2005). Dissection of COPII subunit-cargo assembly and disassembly kinetics during Sar1p-GTP hydrolysis. *Nat. Struct. Mol. Biol.* **12**, 167–74.
Sauvageau, E., Rochdi, M. D., Oueslati, M., Hamdan, F. F., Percherancier, Y., Simpson, J. C., Pepperkok, R. and Bouvier, M. (2014). CNIH4 Interacts with Newly Synthesized GPCR and Controls Their Export from the Endoplasmic Reticulum. *Traffic* **15**, 383–400.
Schlacht, A. and Dacks, J. B. (2015). Unexpected Ancient Paralogs and an Evolutionary Model for the COPII Coat Complex. *Genome Biol Evol* **7**, 1098–109.
Schwarz, K., Iolascon, A., Verissimo, F., Trede, N. S., Horsley, W., Chen, W., Paw, B. H., Hopfner, K.-P. P., Holzmann, K., Russo, R., et al. (2009). Mutations affecting the secretory COPII coat component SEC23B cause congenital dyserythropoietic anemia type II. *Nat. Genet.* **41**, 936–40.
Seifert, J. R. and Mlodzik, M. (2007). Frizzled/PCP signalling: a conserved mechanism regulating cell polarity and directed motility. *Nat. Rev. Genet.* **8**, 126–38.
Shimoni, Y., Kurihara, T., Ravazzola, M., Amherdt, M., Orci, L. and Schekman, R. (2000). Lst1p and Sec24p cooperate in sorting of the plasma membrane ATPase into COPII vesicles in Saccharomyces cerevisiae. *J. Cell Biol.* **151**, 973–84.
Shum, L., Turck, C. W. and Derynck, R. (1996). Cysteines 153 and 154 of transmembrane transforming growth factor-alpha are palmitoylated and mediate cytoplasmic protein association. *The Journal of biological chemistry* **271**, 28502–8.
Simons, M. and Mlodzik, M. (2008). Planar cell polarity signaling: from fly development to human disease. *Annu. Rev. Genet.* **42**, 517–40.

Strong, L. C. and Hollander, W. F. (1949). Hereditary loop-tail in the house mouse. *Journal of Heredity* **40**, 329–334.
Tao, J., Zhu, M., Wang, H., Afelik, S., Vasievich, M. P., Chen, X.-W. W., Zhu, G., Jensen, J., Ginsburg, D. and Zhang, B. (2012). SEC23B is required for the maintenance of murine professional secretory tissues. *Proc. Natl. Acad. Sci. U.S.A.* **109**, E2001–9.
Taylor, J., Abramova, N., Charlton, J. and Adler, P. N. (1998). Van Gogh: a new Drosophila tissue polarity gene. *Genetics* **150**, 199–210.
Teixidó, J. and Massagué, J. (1988). Structural properties of a soluble bioactive precursor for transforming growth factor-alpha. *J. Biol. Chem.* **263**, 3924–9.
Teixidó, J., Gilmore, R., Lee, D. C. and Massagué, J. (1987). Integral membrane glycoprotein properties of the prohormone pro-transforming growth factor-alpha. *Nature* **326**, 883–5.
Todaro, G. J., Larco, J. E. De and Cohen, S. (1976). Transformation by murine and feline sarcoma viruses specifically blocks binding of epidermal growth factor to cells. *Nature* **264**, 26–31.
Ureña, J. M., Merlos-Suárez, A., Baselga, J. and Arribas, J. (1999). The cytoplasmic carboxy-terminal amino acid determines the subcellular localization of proTGF-(alpha) and membrane type matrix metalloprotease (MT1-MMP). *J. Cell. Sci.* **112 (Pt 6)**, 773–84.
Usui, T., Shima, Y., Shimada, Y., Hirano, S., Burgess, R. W., Schwarz, T. L., Takeichi, M. and Uemura, T. (1999). Flamingo, a seven-pass transmembrane cadherin, regulates planar cell polarity under the control of Frizzled. *Cell* **98**, 585–95.
Vinson, C. R. and Adler, P. N. (1987). Directional non-cell autonomy and the transmission of polarity information by the frizzled gene of Drosophila. *Nature* **329**, 549–51.
Wallingford, J. B., Rowning, B. A., Vogeli, K. M., Rothbächer, U., Fraser, S. E. and Harland, R. M. (2000). Dishevelled controls cell polarity during Xenopus gastrulation. *Nature* **405**, 81–5.
Wang, Y., Guo, N. and Nathans, J. (2006a). The role of Frizzled3 and Frizzled6 in neural tube closure and in the planar polarity of inner-ear sensory hair cells. *J. Neurosci.* **26**, 2147–56.
Wang, J., Hamblet, N. S., Mark, S., Dickinson, M. E., Brinkman, B. C., Segil, N., Fraser, S. E., Chen, P., Wallingford, J. B. and Wynshaw-Boris, A. (2006b). Dishevelled genes mediate a conserved mammalian PCP pathway to regulate convergent extension during neurulation. *Development* **133**, 1767–78.
Wansleeben, C., Feitsma, H., Montcouquiol, M., Kroon, C., Cuppen, E. and Meijlink, F. (2010). Planar cell polarity defects and defective Vangl2 trafficking in mutants for the COPII gene Sec24b. *Development* **137**, 1067–73.
Wawrzyniak, A. M., Vermeiren, E., Zimmermann, P. and Ivarsson, Y. (2012). Extensions of PSD-95/discs large/ZO-1 (PDZ) domains influence lipid binding and membrane targeting of syntenin-1. *FEBS Lett.* **586**, 1445–51.
Wendeler, M. W., Paccaud, J.-P. P. and Hauri, H.-P. P. (2007). Role of Sec24 isoforms in selective export of membrane proteins from the endoplasmic reticulum. *EMBO Rep.* **8**, 258–64.

Williams, T. A., Foster, P. G., Cox, C. J. and Embley, T. M. (2013). An archaeal origin of eukaryotes supports only two primary domains of life. *Nature* **504**, 231–6.
Wolff, T. and Rubin, G. M. (1998). Strabismus, a novel gene that regulates tissue polarity and cell fate decisions in Drosophila. *Development* **125**, 1149–59.
Yang, X.-Y. Y., Zhou, X.-Y. Y., Wang, Q. Q., Li, H., Chen, Y., Lei, Y.-P. P., Ma, X.-H. H., Kong, P., Shi, Y., Jin, L., et al. (2013). Mutations in the COPII vesicle component gene SEC24B are associated with human neural tube defects. *Hum. Mutat.* **34**, 1094–101.
Yu, H., Ye, X., Guo, N. and Nathans, J. (2012). Frizzled 2 and frizzled 7 function redundantly in convergent extension and closure of the ventricular septum and palate: evidence for a network of interacting genes. *Development* **139**, 4383–94.